MAY 14 1963

MMPP – NPC – I – 4

MICHIGAN MEMORIAL PHOENIX PROJECT
THE UNIVERSITY OF MICHIGAN

MASTER

Facsimile Price $ 5.60
Microfilm Price $ 1.23

Available from the
Office of Technical Services
Department of Commerce
Washington 25, D. C.

LATTICE WAVES, SPIN WAVES AND NEUTRON SCATTERING

By B. N. BROCKHOUSE
CHALK RIVER PROJECT
ATOMIC ENERGY OF CANADA LIMITED

A PAPER BASED ON LECTURES PRESENTED AT
THE NEUTRON PHYSICS CONFERENCE
MACKINAC ISLAND, MICHIGAN
JUNE 12–17, 1961

LEGAL NOTICE

This report was prepared as an account of Government sponsored work. Neither the United States, nor the Commission, nor any person acting on behalf of the Commission:

A. Makes any warranty or representation, expressed or implied, with respect to the accuracy, completeness, or usefulness of the information contained in this report, or that the use of any information, apparatus, method, or process disclosed in this report may not infringe privately owned rights; or

B. Assumes any liabilities with respect to the use of, or for damages resulting from the use of any information, apparatus, method, or process disclosed in this report.

As used in the above, "person acting on behalf of the Commission" includes any employee or contractor of the Commission, or employee of such contractor, to the extent that such employee or contractor of the Commission, or employee of such contractor prepares, disseminates, or provides access to, any information pursuant to his employment or contract with the Commission, or his employment with such contractor.

ANN ARBOR MICHIGAN

DISCLAIMER

Portions of this document may be illegible in electronic image products. Images are produced from the best available original document.

LATTICE WAVES, SPIN WAVES AND NEUTRON SCATTERING

by

B. N. BROCKHOUSE

Chalk River Project
Atomic Energy of Canada Limited

A Paper Based on

Lectures Presented at

The Neutron Physics Conference

Mackinac Island, Michigan

June 12-17, 1961

The Neutron Physics Conference of 1961 was sponsored by the

UNITED STATES ATOMIC ENERGY COMMISSION,

LEAR, INCORPORATED,

DETROIT EDISON COMPANY,

CONDUCTRON CORPORATION,

and by the

INSTITUTE OF SCIENCE AND TECHNOLOGY,

ENGINEERING SUMMER CONFERENCE PROGRAM,

and MICHIGAN MEMORIAL PHOENIX PROJECT

of THE UNIVERSITY OF MICHIGAN.

Preface

At the Neutron Physics Conference in June 1961, four lectures on experiments in neutron spectrometry were given in the general series and a fifth in an extra session on scattering of neutrons by liquids. No formal manuscripts for these talks were prepared, and the lectures involved such a large number of slides that it was thought better to publish an abridged version. The following paper was actually prepared for delivery as the Oliver E. Buckley Lecture at the Baltimore Meeting of the American Physical Society in March 1962. The material given in it was included also in the lectures at the Neutron Physics Conference, except for the very recent results (Figure 22) of Dr. H. Watanabe and myself on the spin wave dispersion curves in magnetite.

A review article covering other aspects of the subject will appear in the volume Materials Science Lectures edited by E. Leonard Jossem, to be published by the Ohio State University Press. Reference can also be made to the volume of conference papers Inelastic Scattering of Neutrons in Solids and Liquids, published in 1961 by the International Atomic Energy Agency, Vienna.

B. N. Brockhouse

It was recognized many years ago that study of neutron inelastic scattering would yield a variety of information not easily obtained in other ways. The first measurements were reported from Cambridge University in 1947 by Cassels and Latham[1] who studied the total cross section of iron (and later of other materials) and drew inferences about the lattice waves in the form of "Debye" temperatures. The first crude studies of the energy distributions were made about 1951, using absorption methods, by Egelstaff[2] at Harwell and by D. G. Hurst and myself at Chalk River[3]. All these experiments were qualitative only; they were valuable at the time as tests of the neutron scattering theory but gave no essentially new information about the specimen itself.

In 1952 a spectrometer was set up at the NRX reactor at Chalk River to measure actual energy distributions. Before the experiments gave any definite results, the "lamp" burned out---the reactor had an accident. When it was turned on again about eighteen months later, the spectrometer was set up once more, and studies[4] of energy distributions have been carried on from August 1954 till the present time, almost without interruption.

The first experiments were again qualitative. Among other things, the experiments verified the existence of the quantum of lattice vibrations---the phonon---and the quantum of spin waves---the magnon---in a striking and decisive way.

The scattered neutrons energy distributions could be interpreted,

intuitively, as the result of collisions between the neutrons and entities---the phonons and magnons---having definite energies and momenta, energy and momentum being conserved in the collisions. This, of course, was as predicted by existing theory.

Since about 1957 the experiments have been in a new phase in which accurate experiments are yielding reliable information about the forces between the atoms in solids and in liquids. Although the results for liquids are highly interesting, my talk will be restricted to the studies of solids, and in particular to one class of experiments in solids: experiments which yield in a very direct way the dispersion relation between the frequency and the wave length of the lattice vibrations, or of the spin waves, in a crystal.

Now one may ask: "Why are neutrons so useful in the experiments? Why not use some other radiation, say X-rays or infrared?" The answer lies in the relation between the energy and the momentum of the neutron; that is between its energy and its wave length. Neutrons emerge from a reactor with an approximately Maxwellian spectrum at a temperature slightly higher than the temperature of the moderator, which in turn is usually somewhat higher than room temperature. Thus, the spectrum might be somewhat as shown in Figure 1. Room temperature neutrons with energies of 25 millivolts have wave lengths of about 1.8 Å; those with energies of one-tenth of a volt have wave lengths of about nine-tenths of an angstrom. Thus, neutrons have simultaneously energies of the

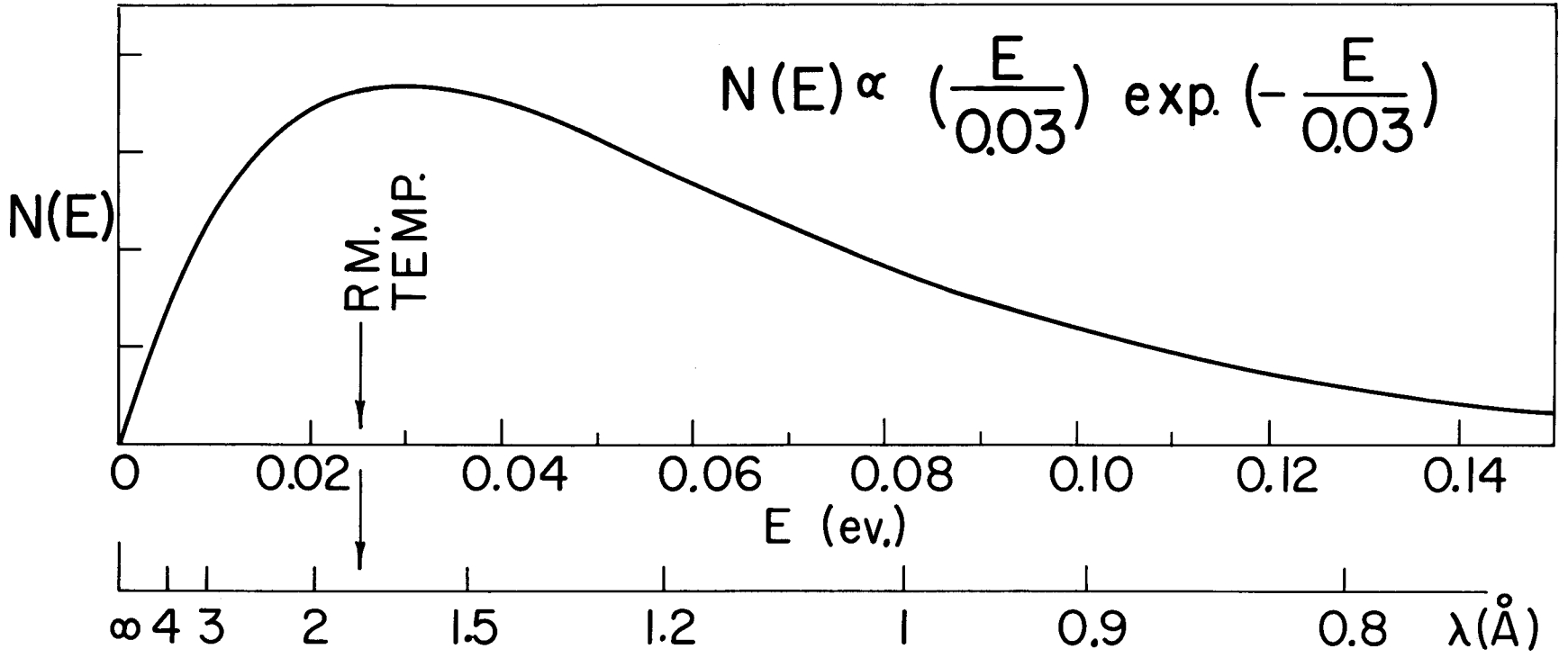

X-RAYS : $\lambda = 1.8$ Å $\longleftrightarrow$ $E \simeq 7000$ ev.

INFRA-RED : $E = 0.025$ ev. $\longleftrightarrow$ $\lambda \simeq 5 \times 10^5$ Å

Figure 1

order of the characteristic energies in solids and liquids and wave lengths of the order of interatomic spacings. On the other hand, X-rays with wave length 1.8 Å have energies of about 7000 volts, many orders of magnitude larger than the characteristic energies, while room temperature infrared radiation has a wave length of five hundred thousand angstroms. Thus, with X-rays, one cannot get high enough resolution to measure energy distributions, while with infrared, one can see only atomic motions in which very large numbers of atoms move together as a group. With neutrons one is able to see disturbances of almost any wave length or energy likely to occur.

In the experiments, one selects from the spectrum a narrow, substantially monoenergetic, beam of neutrons. The neutrons scatter from the specimen and are observed at different angles; their energies after scattering are measured by a spectrometer. The initial and final energy selections may be made either by Bragg reflection by a crystal or by measurement of the time of flight of the neutrons over a known path length.

Figure 2 shows an actual experimental set-up. White neutrons from the pile fall on the monochromating crystal. Neutrons of the desired wave length are Bragg reflected from the monochromator and impinge on the specimen. Scattered neutrons are observed at some angle ϕ, and their energies are measured by Bragg reflection from the analyzing crystal. The wave lengths are determined from the angles $2\theta_M$ and $2\theta_A$ using the Bragg law.

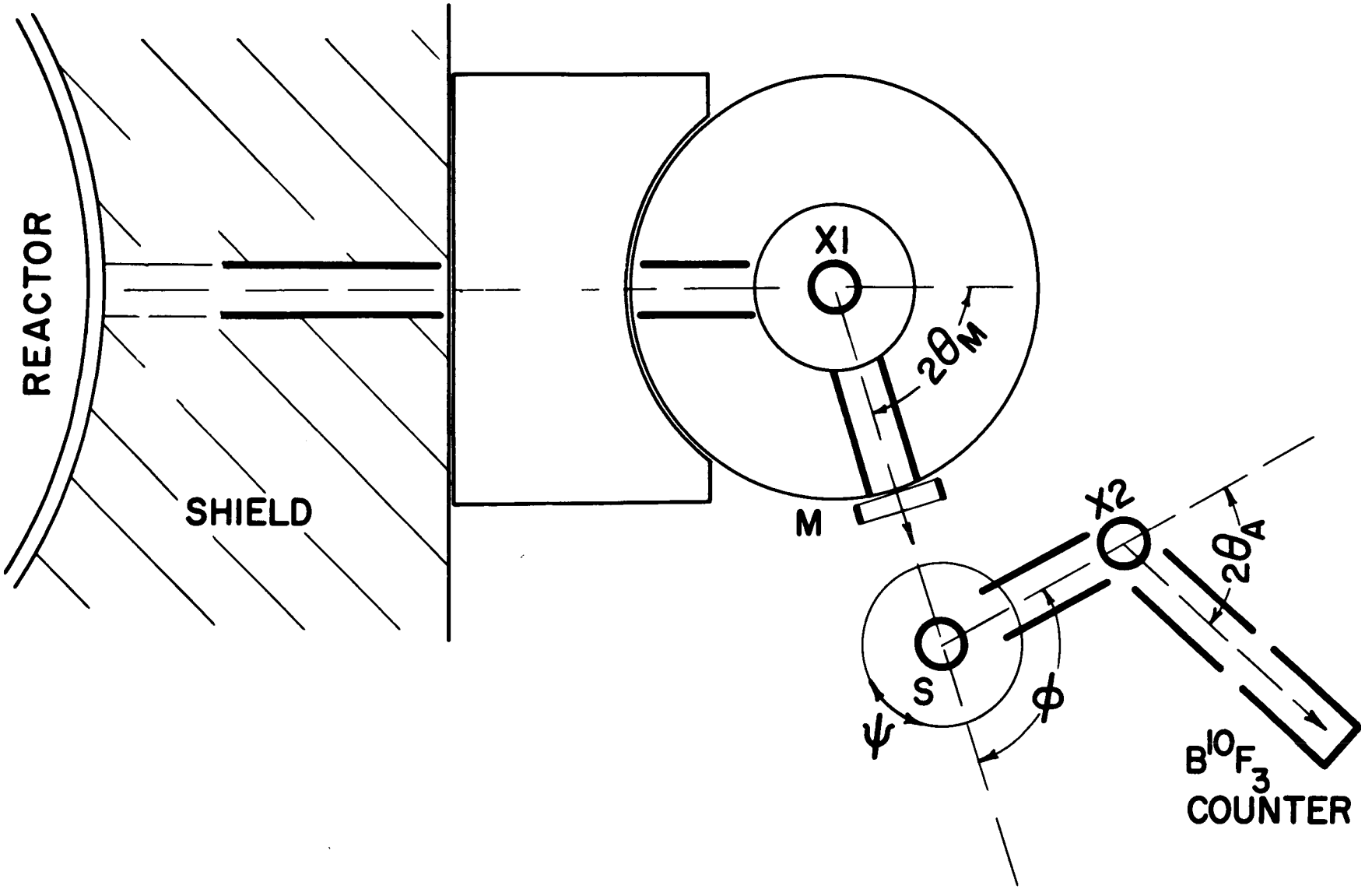
REACTOR
SHIELD
X1
M
$2\theta_M$
X2
$2\theta_A$
S
ψ
ϕ
$B^{10}F_3$
COUNTER

Figure 2

It is convenient to begin by discussing the Bragg law, the conditions on elastic coherent scattering[5] by a crystal. The Bragg law may be written as shown in Figure 3. The difference between the incoming and outgoing neutron wave vectors is equal to a vector ($\underset{\sim}{\tau}$) of the reciprocal lattice. The vector $\underset{\sim}{\tau}$ is a vector normal to the reflecting planes and having a length any integer (n) times the reciprocal of the spacing (d) between the planes. The scattering is elastic, so the energy transfer is zero. The wave vectors $\underset{\sim}{k}$ have magnitudes as defined and directions in the direction of propagation of the neutron.

The termini of the vectors $\underset{\sim}{\tau}$ form the <u>reciprocal lattice</u>, and the Bragg law can be displayed graphically as the <u>Ewald construction</u>. The Bragg law is satisfied when one can draw incoming and outgoing vectors (of equal length) in such a way that $\underset{\sim}{k}_o$ begins on a reciprocal lattice point and $-\underset{\sim}{k}'$ ends on another.

In Bragg scattering the quantum numbers of the crystal are unchanged in the scattering process. We now consider the <u>one-phonon</u> process, in which the quantum numbers of <u>one</u> of the normal modes of the crystal are increased or decreased by one. Then if the normal mode considered has a frequency ν and wave vector $\underset{\sim}{q}$, the one phonon scattering is described[5] by the interference or momentum conservation condition:

$$\underset{\sim}{k}_o - \underset{\sim}{k}' = 2\pi\underset{\sim}{\tau} - \underset{\sim}{q}$$

EWALD CONSTRUCTION

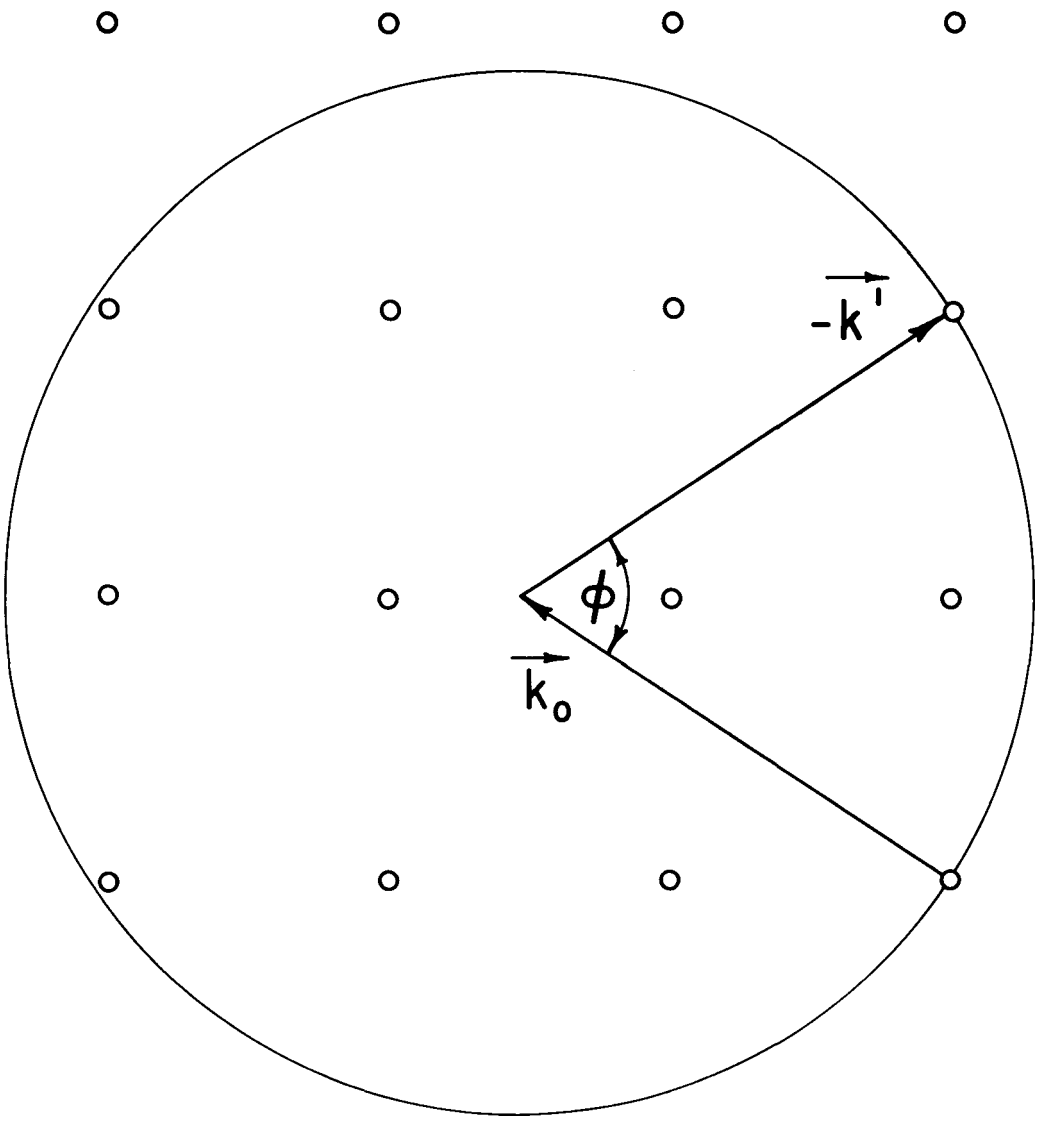

BRAGG LAW

$$\vec{k}_0 - \vec{k}' = 2\pi\vec{\tau}$$

$$E_0 - E' = 0$$

$$\vec{\tau} = \left(\frac{\vec{n}}{d}\right)$$

$$E = \frac{\hbar^2 k^2}{2 m_N}$$

$$k = \frac{2\pi}{\lambda}$$

Figure 3

and the energy conservation condition:

$$E_o - E' = \pm h\nu.$$

The interference condition can be displayed in the reciprocal lattice as a generalized Ewald construction; in this case the two vectors are not of equal length, their lengths are determined by the energy conservation conditions.

The lattice vibrations[6] fall into branches. For each wave vector q there are 3n vibrations where n is the number of atoms in the primitive unit cell; the number 3 comes from the three possible orthogonal directions of polarization in space. The lattice vibrations have the symmetry of the reciprocal lattice: the frequency repeats over reciprocal space, and we need consider only the frequencies within a single zone about a reciprocal lattice point, the frequencies in other zones being identical. Thus, along a horizontal line through a series of reciprocal lattice points, the frequency of a particular branch might vary with q as shown by the solid curve in Figure 4. Along the line of our vector $-\underset{\sim}{k}'$, the frequency might vary as shown by the dashed curve. There is thus a three dimensional dispersion relation for each branch (j); $\nu = \nu_j(\underset{\sim}{q})$, where $\underset{\sim}{q}$ is defined only over one zone of reciprocal space centered about the reciprocal lattice points, and the dispersion relation repeats over reciprocal space.

Figure 4

A.E.C.L. Ref. # A-2782-H

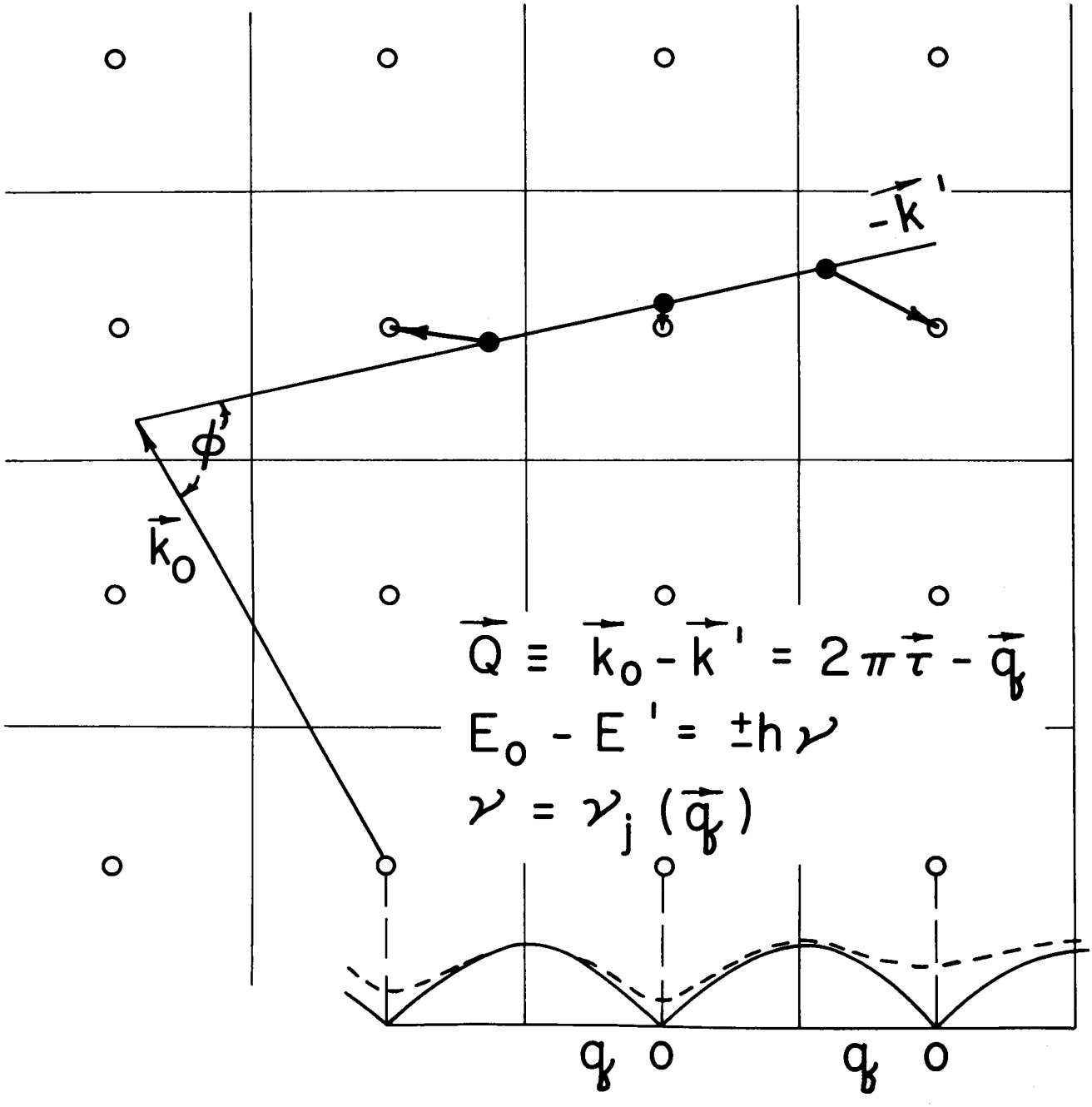

We recognize neutrons scattered in the one phonon process by the fact that they occur <u>in groups</u> in the energy and angular distributions. We have four unknowns, the three components of $\underset{\sim}{q}$ and the frequency, and we have five equations. Thus, we have five equations in four unknowns, and solutions can occur but rarely. The neutrons occur in groups corresponding to the solutions.

In the experiment shown graphically in Figure 4, we might find three groups corresponding to one phonon scattering from the branch shown, two in energy gain (phonon annihilation) and one in energy loss (phonon creation). The centers of the groups would give us the frequency by energy conservation, and the wave vector by completing to the nearest reciprocal lattice point. Thus, the experiment shown would yield three points on the dispersion relation. The experiment would then be repeated at different crystal orientations, angles of scattering, and perhaps incident wave lengths, and the dispersion relation built up.

It will be observed that in these experiments the frequency and wave vector are deduced simply from energy and momentum conservation, without the intervention of any very complicated theory.

By measuring the same phonon (with reduced wave vector $\underset{\sim}{q}$) at various equivalent positions in reciprocal space, we are often able to assign[7] the character (i.e. optical or acoustical, longitudinal or transverse) from the intensities of the neutron groups.

Figure 5 shows our first experiments[8], made in early 1955 on an aluminum crystal. At the right are plotted distributions showing the counting rate vs. the setting of the analyzing spectrometer. An auxiliary scale shows the outgoing energy; the incident energy was 63 millivolts. The experiments were carried out at a fixed angle of scattering, the five distributions corresponding to five orientations of the crystal with respect to the incident neutron beam, as shown in the reciprocal lattice diagram at the left in Figure 5. The positions of the centers of the neutron groups are plotted as shown by the code numbers.

Despite the poor resolution, it is clear that neutron groups are observed and that the conservation laws are obeyed. Experiments such as these put the phonon in almost the same category of reality as the experiments on the photoelectric effect and the Compton effect placed the photon.

Figure 6 shows dispersion curves for two symmetric directions in the reduced zone, the cube edge and the face diagonal. The points were obtained from experiments similar in principle to those of Figure 5. Points were obtained by A. T. Stewart and myself at Chalk River[9], and at about the same time, by Carter, Hughes and Palevsky[10] at Brookhaven. Results obtained somewhat later at the Stockholm reactor by Larsson, Dahlborg and Holmryd[11] are also shown. By and large, the neutron results agree well within the rather large errors. Dispersion curves deduced by Walker[12] from X-ray intensity measurements, using an entirely different

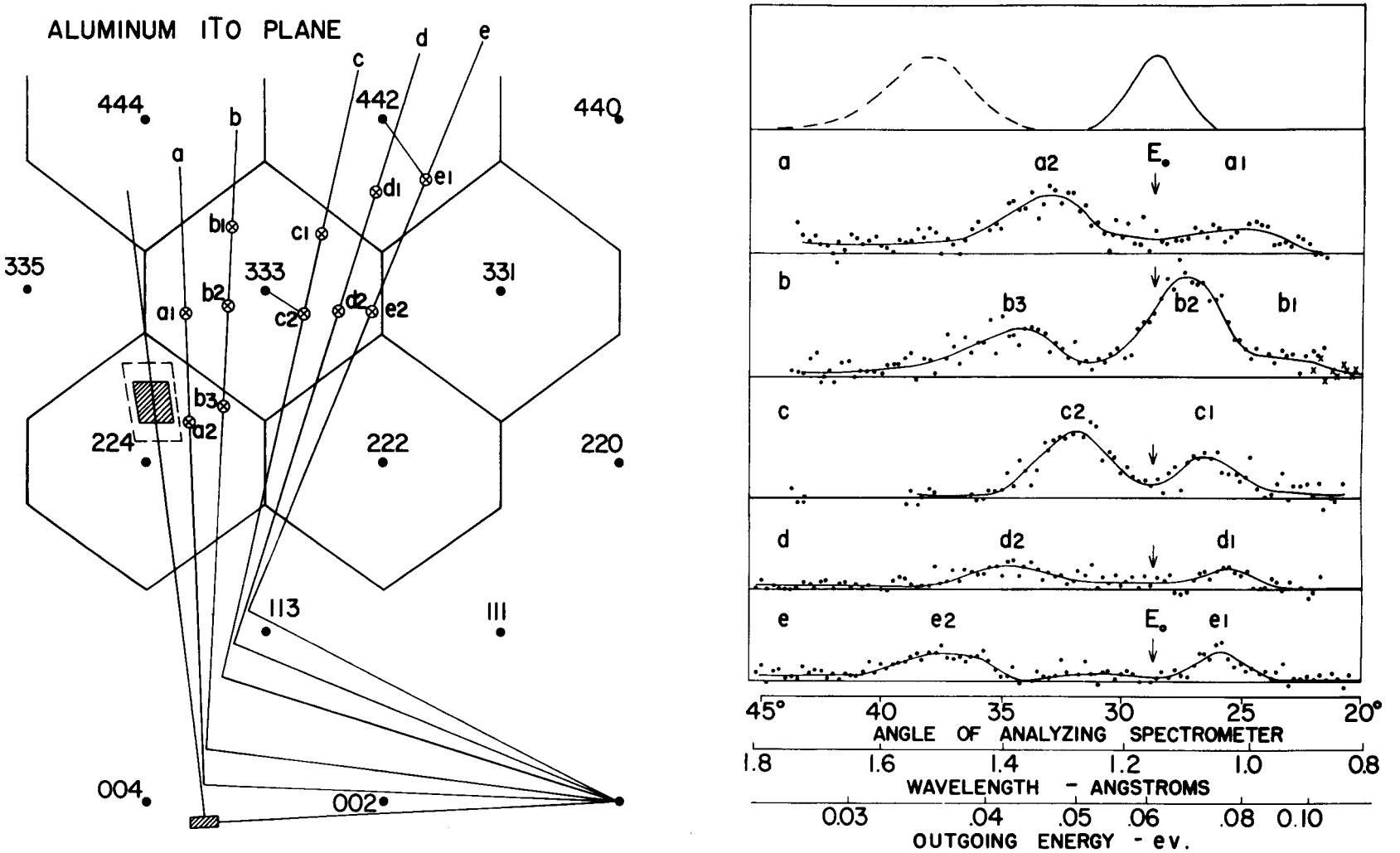
ALUMINUM ITO PLANE
444
440
442
335
331
333
224
222
220
113
111
004
002
a
b
c
d
e
a1
a2
b1
b2
b3
c1
c2
d1
d2
e1
e2
E₀
45°
40
35
30
25
20°
ANGLE OF ANALYZING SPECTROMETER
1.8
1.6
1.4
1.2
1.0
0.8
WAVELENGTH - ANGSTROMS
0.03
.04
.05
.06
.08
0.10
OUTGOING ENERGY - ev.

Figure 5

A.E.C.L. Ref. # A-2563-B

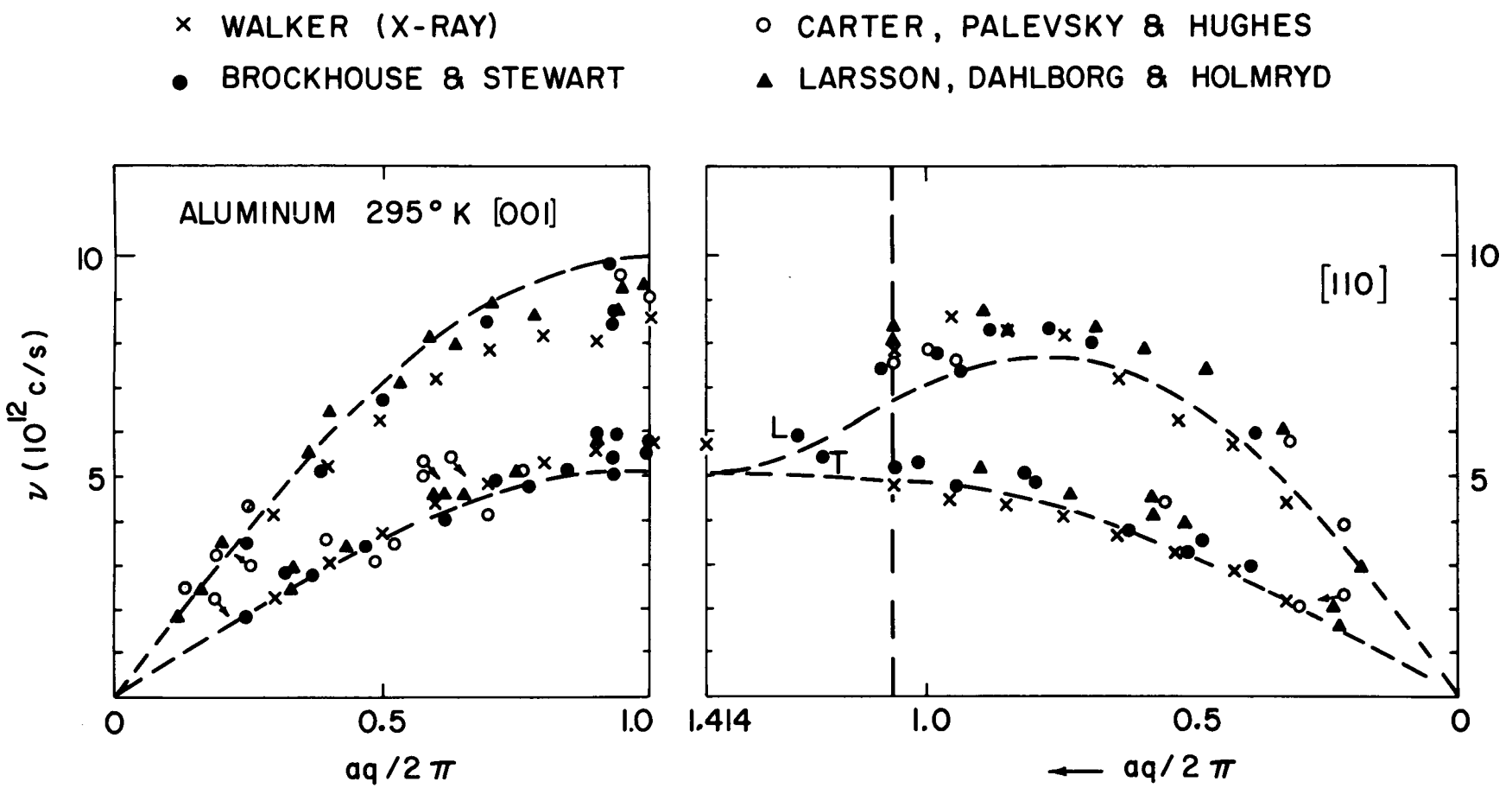

Figure 6

though less direct method, are also shown. Again, the agreement is satisfying, though systematic discrepancies occur.

Dispersion curves such as these are interesting from at least two points of view.

1. Since they describe completely the dynamics of the crystal insofar as it is harmonic, they can be used to compute thermodynamic properties such as the specific heat or electronic transport properties such as the electrical conductivity.
2. Since the dispersion curves are determined by the interatomic forces in the crystal, the experimental results can be analyzed to determine the nature of the interatomic forces.

For me, it is this latter application which is the more interesting.

Dispersion curves computed from measured elastic constants using a force model of Begbie and Born[6] are shown as dashed lines. The model assumes general (non-central) forces between first neighbors in the crystal. The general resemblance is very satisfying if one recalls that no fitting to the neutron results was used. Nevertheless, it is clear that a more complicated model is required.

Figure 7 shows results on germanium[7] obtained in 1957 by P. K. Iyengar and myself. Germanium has two atoms per primitive

Figure 7

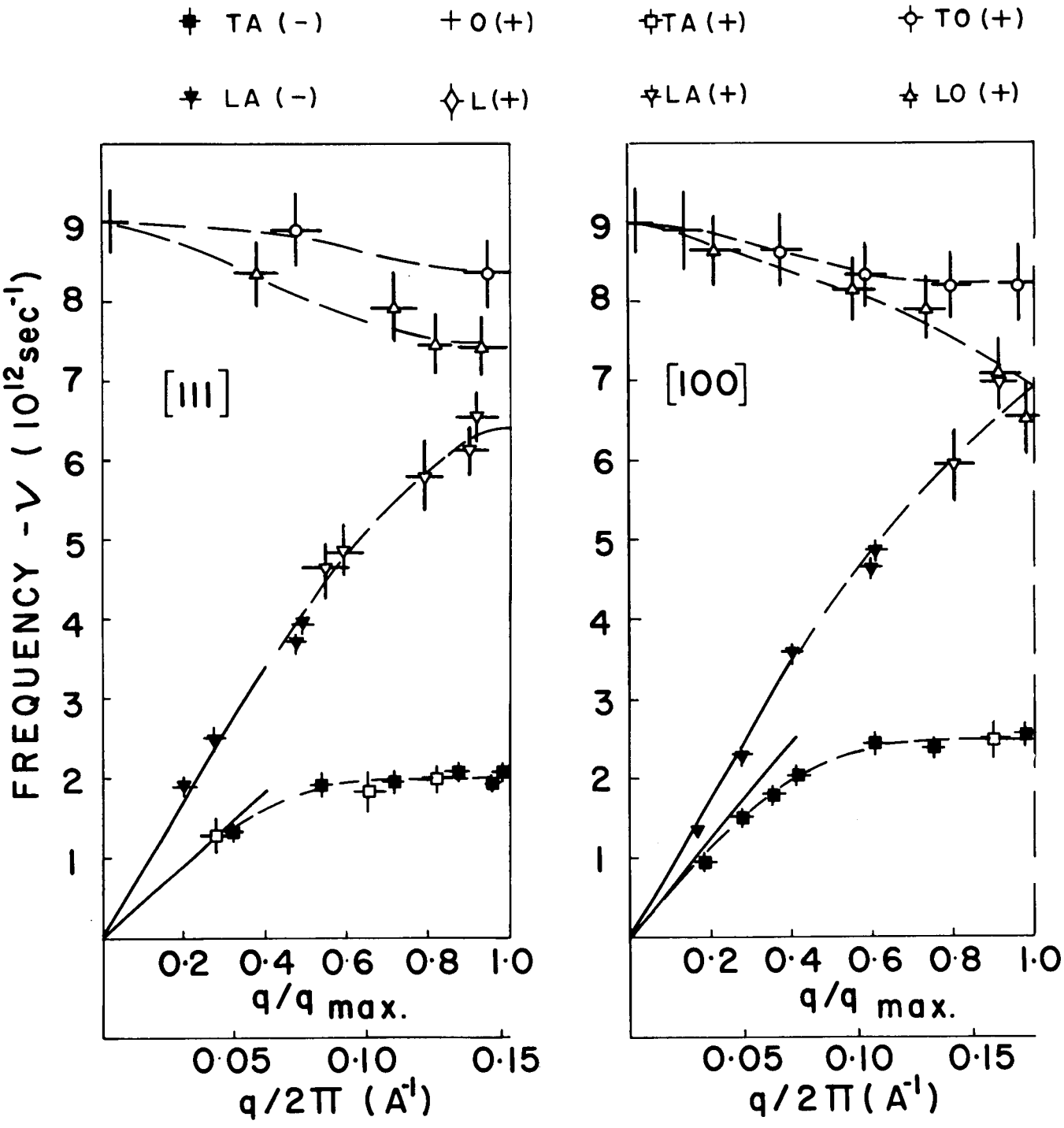
TA (-)
O (+)
TA (+)
TO (+)
LA (-)
L (+)
LA (+)
LO (+)
FREQUENCY - ν (10^12 sec^-1)
[111]
[100]
1
2
3
4
5
6
7
8
9
0·2
0·4
0·6
0·8
1·0
q/q max.
0·05
0·10
0·15
q/2π (A^-1)

unit cell; there are, therefore, six branches to the dispersion relation. In the symmetry directions shown, along the cube edge and the body diagonal, these are: a longitudinal optical branch, a doubly degenerate transverse optical branch, a longitudinal acoustic branch, and a doubly degenerate transverse acoustic branch.

Analysis of the results according to the Born-von Kármán theory[6] showed that a complicated force model involving long range forces between the atoms was required to explain the results. Cochran[13] showed that these long range forces probably are electrostatic forces arising from the mutual polarizabilities of the ions.

These experiments had other interesting results. For one, they laid the basis for a small but currently flourishing field of physics, the interpretation of the multiple phonon bands in the far-infrared spectra of crystals in terms of phonon energies at symmetry points in the crystal.

In Figure 8 is shown the far-infrared absorption coefficient of germanium[14] as a function of the infrared wave length and frequency. There is considerable structure with a fairly intense peak at about 10.4×10^{12} cps; (remember the logarithmic ordinate scale). First order (one-phonon) infrared absorption is forbidden in germanium by symmetry. Higher order (multiple-phonon) processes, however, are allowed. There had been considerable speculation that the sharp peak at 10.4×10^{12} cps was, in fact, the reststrahlen

Figure 8

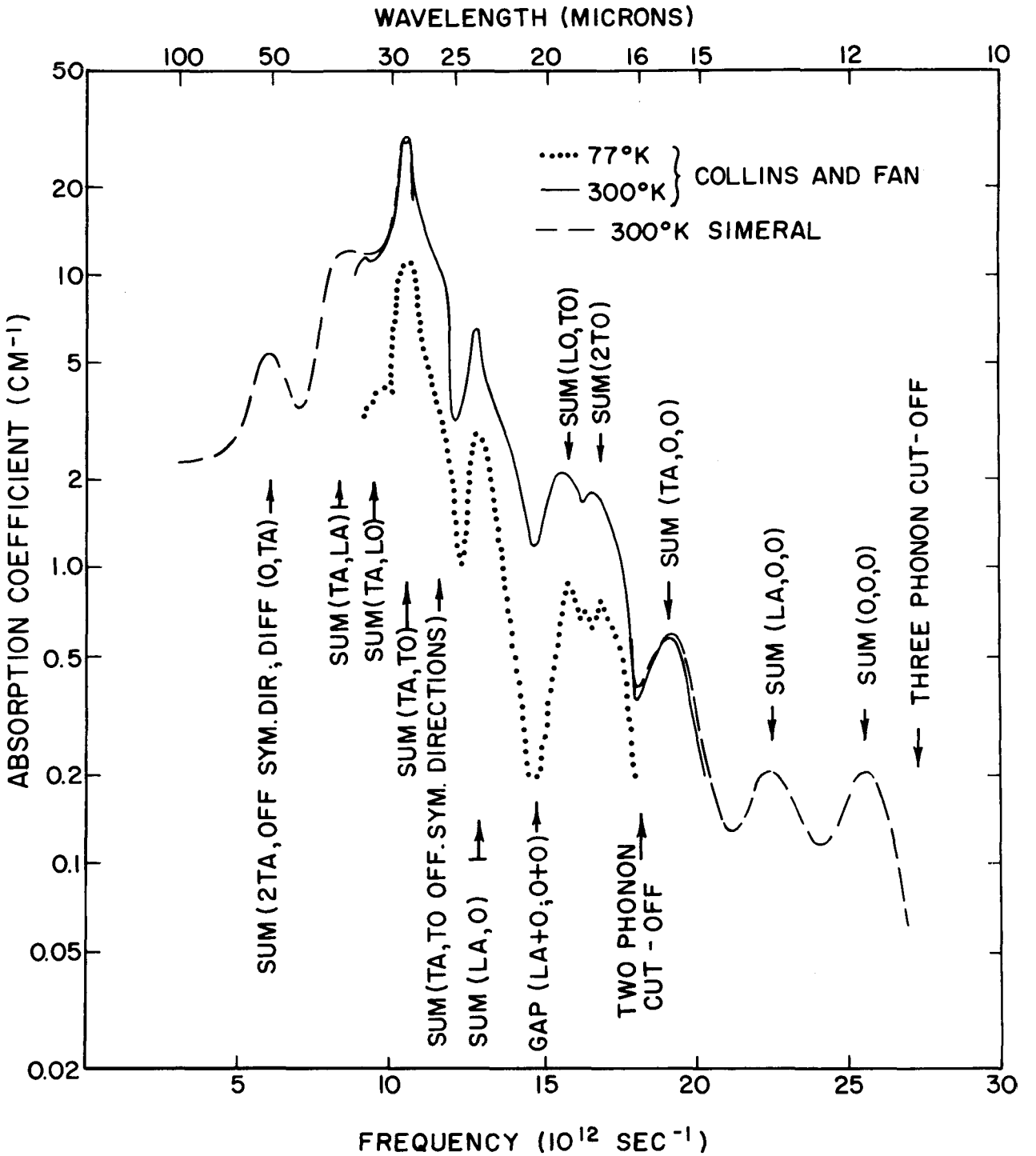
WAVELENGTH (MICRONS)
100
50
30
25
20
16
15
12
10
ABSORPTION COEFFICIENT (CM⁻¹)
50
20
10
5
2
1.0
0.5
0.2
0.1
0.05
0.02
77°K
300°K
COLLINS AND FAN
300°K SIMERAL
SUM (2TA, OFF SYM. DIR.; DIFF (O,TA))
SUM (TA,LA)
SUM (TA,LO)
SUM (TA,TO)
SUM (TA,TO OFF. SYM. DIRECTIONS)
SUM (LA,O)
GAP (LA+O;O+O)
SUM (LO,TO)
SUM (2TO)
TWO PHONON CUT-OFF
SUM (TA,O,O)
SUM (LA,O,O)
SUM (O,O,O)
THREE PHONON CUT-OFF
5
10
15
20
25
30
FREQUENCY (10¹² SEC⁻¹)

frequency, permitted by some small perturbation causing the breakdown of the selection rule against first order one-phonon absorption.

One-phonon absorption occurs for phonons with $\underset{\sim}{q} \simeq 0$, because of the long wave lengths of the infrared radiation. Two-phonon absorption occurs for phonons having the sum of their wave vectors $\underset{\sim}{q}_1 + \underset{\sim}{q}_2 \simeq 0$, and therefore, for phonons with equal but opposite wave vectors.

From the neutron results shown in Figure 7, the optical frequency (at $\underset{\sim}{q} = 0$) is 9.0×10^{12} not the 10.4 of the main infrared peak. However, the sum of the TA and TO frequencies near the zone boundaries is very close to 10.4. It will be observed that the branches are quite flat. Since these are symmetry directions, the frequencies do not change to first order as we go away from the direction (the first derivatives of the frequencies normal to these directions are zero). Therefore, there are large regions of q-space which have substantially the frequencies on these curves. Thus, the intensity and sharpness of the main infrared peak is explained: it arises from two phonon (sum) processes involving the sum of these flat transverse acoustic and transverse optical branches.

Other features of the absorption can also be explained besides this main peak. The highest observed frequency in Figure 7 is the optical frequency at 9×10^{12} cps. Thus, the maximum

frequency in the two-phonon process is 18, and indeed there is a cut-off in the spectrum of Figure 8 at this point. Similarly, the three-phonon cut-off occurs at 27. In fact, every major feature of the absorption curves can be interpreted as combinations of features of the dispersion curves.

Since then the infrared spectra of a considerable number of materials have been analyzed (by other workers) to obtain mean phonon energies at these symmetric regions of reciprocal space.

In the experiments up to 1959 straight forward methods were used. The energy distribution of initially monoenergetic neutrons scattered by a specimen in a fixed orientation through a fixed angle of scattering was studied.

Suppose we wish to measure the frequency of a phonon at the zone boundary in the (111) direction of the reduced zone. Referring to Figure 9, we could select the point B in reciprocal space, set up the experiment as shown, and measure the energy distribution, that is, the length of $-\underset{\sim}{k}'$. We have no assurance that a neutron group would appear at B, instead one might appear at B'. Then we would have to set up new experiments until the group appeared at B, or until the frequency at B could be obtained by interpolation.

We can improve matters by arranging things so that the vector $-\underset{\sim}{k}'$ lies nearly along a direction in which we are interested. Then any neutron group observed will probably be close enough to the desired direction to be interesting.

A.E.C.L. Ref. # A-2606-G

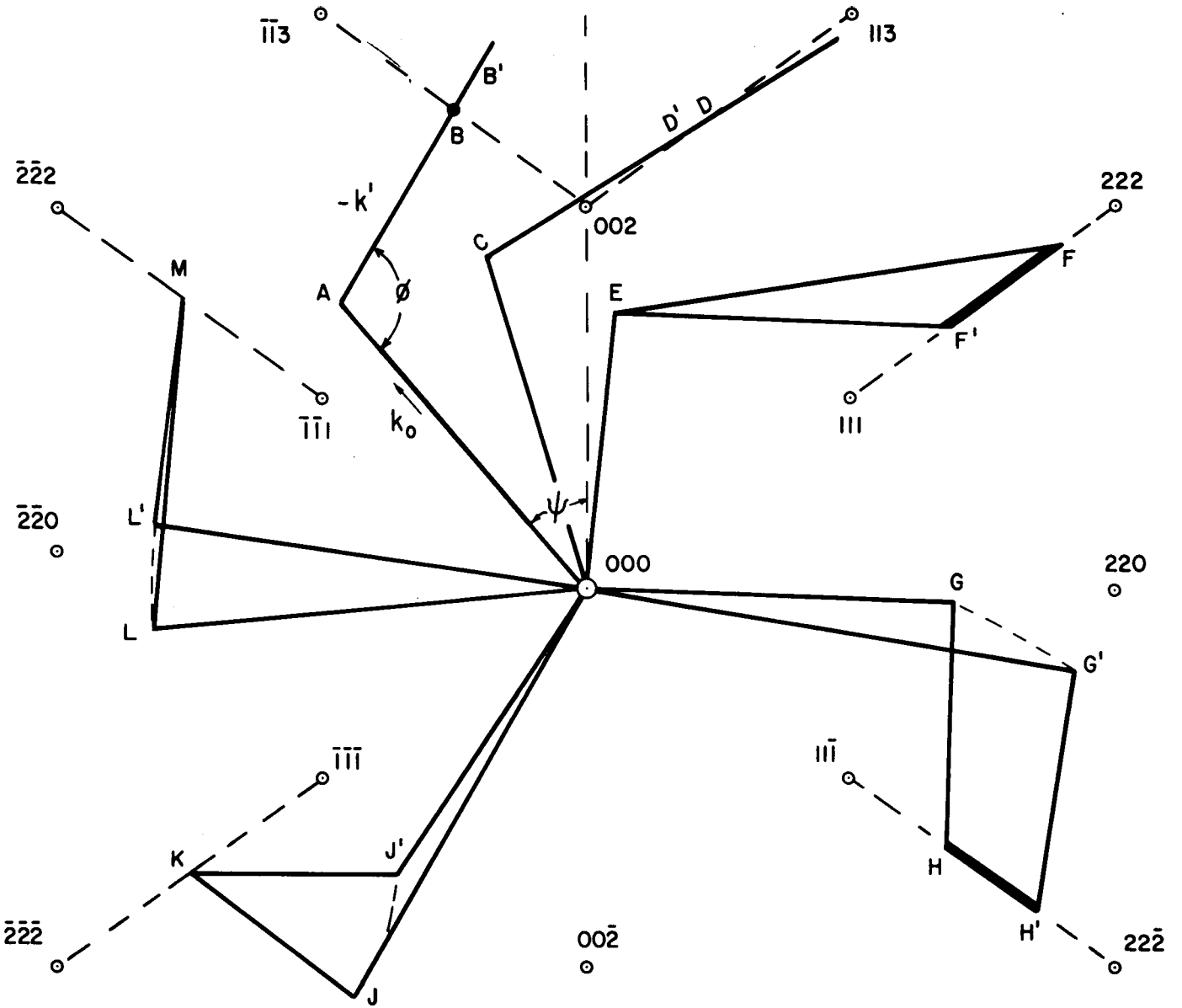

Figure 9

These experiments are unusual in that they are parametric experiments. We wish to measure the dispersion function $\nu(\underset{\sim}{q})$, but the straightforward experiments permit us to obtain only a pair of values, say ν_1 and q_1, which are themselves functions of the actual independent variables.

More sophisticated experiments[15] allow us to study exactly the regions in reciprocal space in which we are interested. Suppose we wish to study the line in reciprocal space F to F'. If, as we change the analyzing spectrometer setting (that is the length of $\underset{\sim}{k}'$) we simultaneously change the angle of scattering by the correct amount, we can arrange to stay in the desired direction. If, furthermore, we also change the orientation of the crystal, we can arrange to stay at the same <u>point</u> in reciprocal space and actually take an energy distribution at the particular wave vector in which we are interested.

Other variations can also be performed. Because the incoming and outgoing neutron energies and wave vectors enter symmetrically in the controlling equations, we can reverse matters and use a fixed analyzer and variable incoming energy. This has technical advantages.

To achieve these more sophisticated experiments, we use a spectrometer in which the various angles (Figure 2) are independently and electrically controlled. The incoming energy is set by the angle $2\theta_M$, the outgoing energy by $2\theta_A$. These, as well as the

angle of scattering ϕ and the crystal orientation ψ, are driven according to instructions printed by a computer on punched paper tape. The computer calculates the parameters needed to achieve the desired series of vector diagrams in a particular experiment using a program designed for that class of experiments.

Figure 9 shows at the bottom left (diagram OJK) the most generally used of the methods, the "constant $\underset{\sim}{Q}$'" or constant momentum transfer method. The analyzer is set to detect neutrons of a selected energy. The incoming neutron energy is changed through the spectrum, the angles of scattering and of crystal orientation being simultaneously (and non-linearly) adjusted so that we remain at the same position in reciprocal space. Thus, we are able to take energy distributions at a particular point $\underset{\sim}{Q}$ in reciprocal space.

From an experimental point of view, this may seem a complicated procedure. From a theoretical point of view, however, the constant momentum transfer experiment is the natural experiment. Quite generally, the only quantities of much interest in neutron scattering from <u>any system</u> are the momentum and energy transfers.

Most of the remaining discussion will be on a series of experiments done over the last three years in collaboration with Dr. A. D. B. Woods and a number of scientists on the crystal dynamics of metals[16-20].

At the left of Figure 10, we see a series of neutron groups obtained[17] with a lead crystal at 100°K using the constant $\underset{\sim}{Q}$ method, at points along the line (1,1,1) to (2,2,2) in reciprocal space. In this direction, the momentum transfer is in the direction of the reduced wave vector; thus, only longitudinal modes should be seen (since in transverse modes the atoms are moving normally to the direction of momentum transfer). At each Q, we obtain an energy distribution which can be plotted directly in terms of frequency. The center of the distribution gives the frequency.

The frequencies should be the same in all zones; in this case, we should be able to fold the curve about the zone boundary.

The dispersion curves[18] in the symmetry directions of the reduced zone for lead at 100°K are shown in Figure 11. This work was done in collaboration with Dr. Woods, T. Arase, G. Caglioti and K. R. Rao. Results are shown for the cube edge, the body diagonal, the face diagonal, and a fourth symmetry direction on the square face of the Brillouin zone. We use this nomenclature in order to be able to include directions which do not pass through the origin of the zone.

The points (1,0,0) and (1,1,0) are equivalent, and the figure shows the various ways in which the different directions join together in reciprocal space. The zone boundary in the (3,3,0) direction is actually at the place indicated; the extension (actually on the square face of the Brillouin zone) has the same

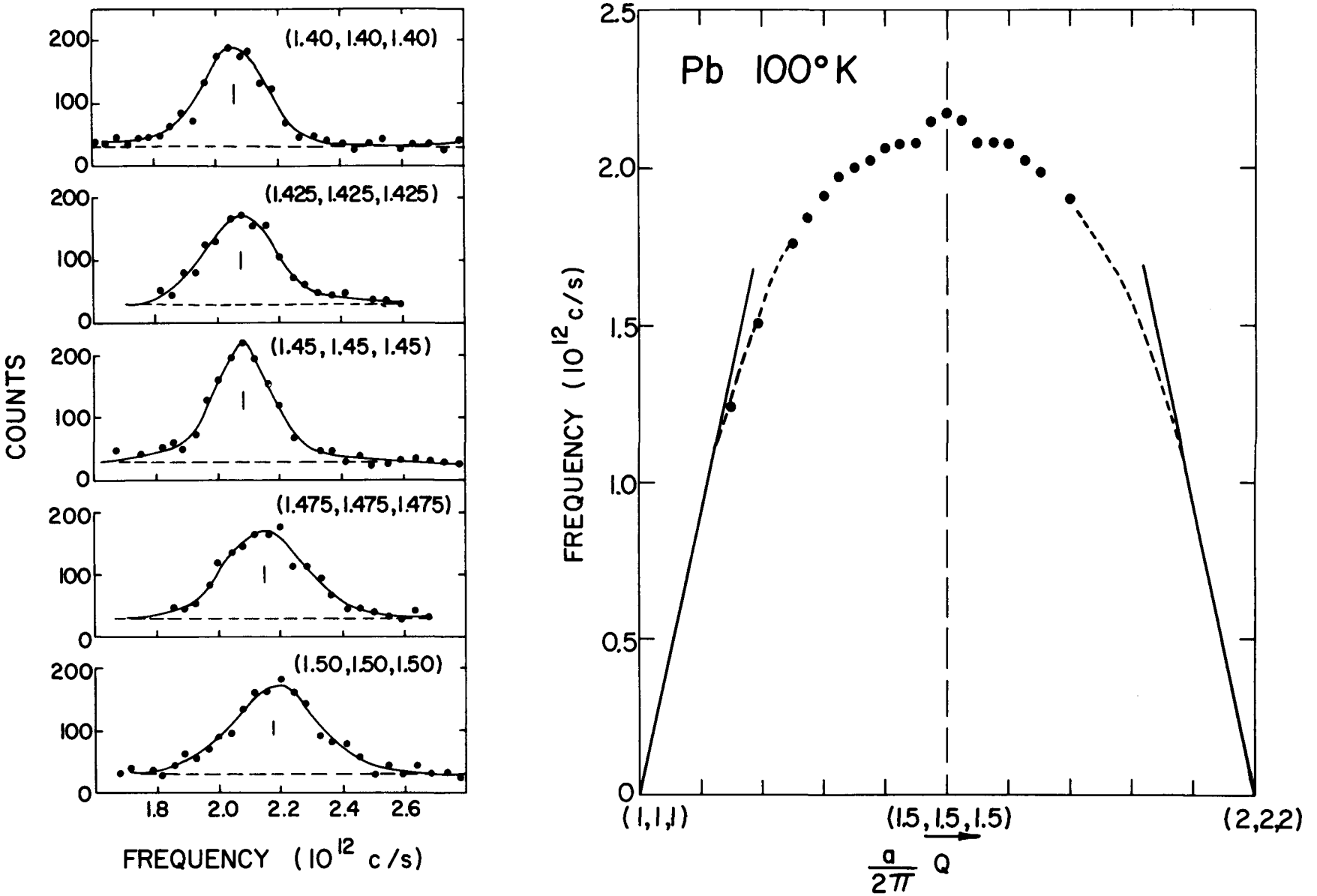
(1.40, 1.40, 1.40)
(1.425, 1.425, 1.425)
(1.45, 1.45, 1.45)
(1.475, 1.475, 1.475)
(1.50, 1.50, 1.50)
COUNTS
200
100
0
1.8
2.0
2.2
2.4
2.6
FREQUENCY (10^{12} c/s)
Pb 100° K
FREQUENCY (10^{12} c/s)
2.5
2.0
1.5
1.0
0.5
0
(1,1,1)
(1.5,1.5,1.5)
(2,2,2)
$\frac{a}{2\pi}$ Q

Figure 10

Figure 11

DISPERSION CURVES OF LEAD AT 100° K

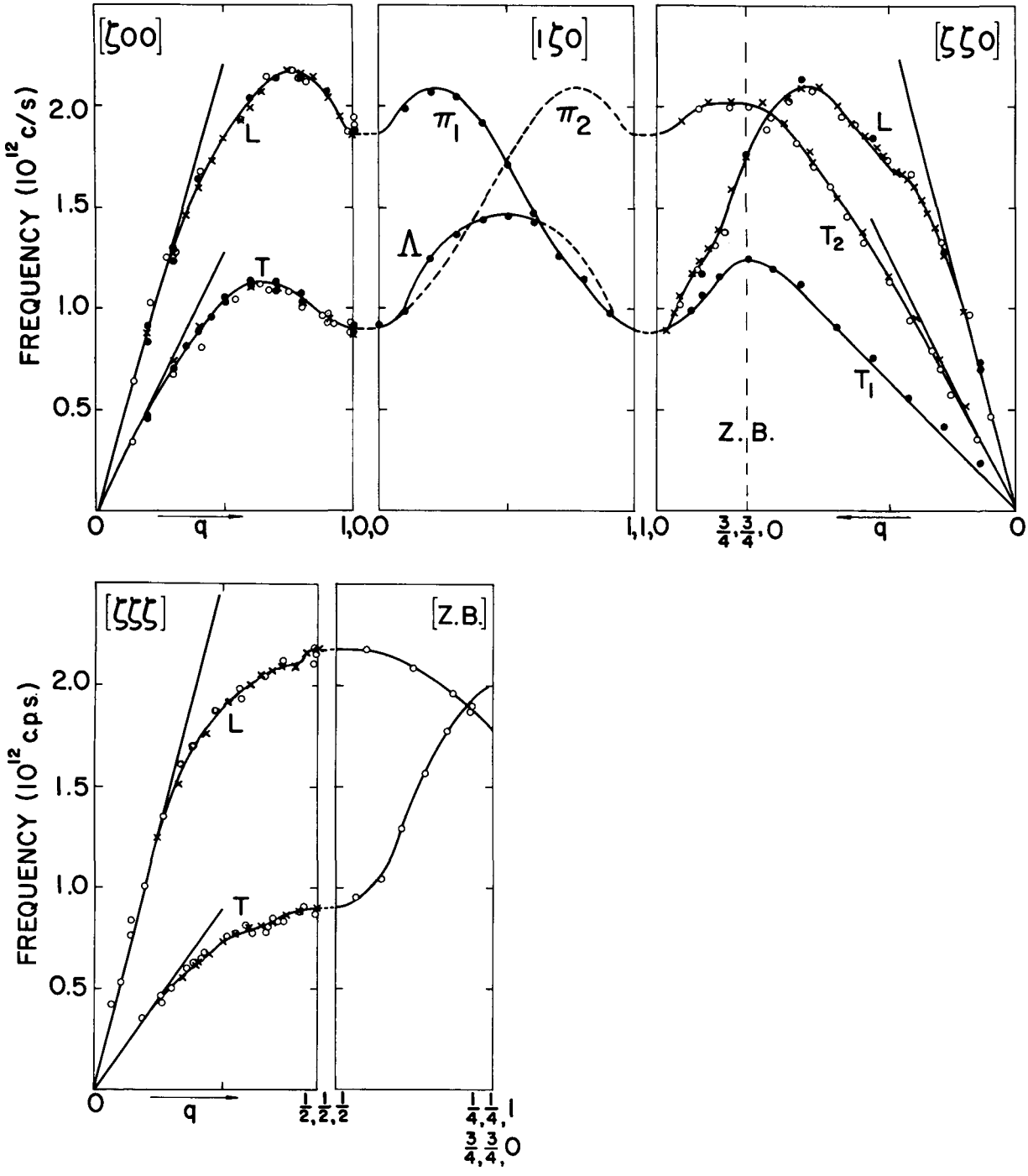

symmetry properties and is continuous with it. We also show the (non-symmetric) boundary direction on the hexagonal face of the Brillouin zone.

Many unusual features exist in these dispersion curves. For one thing, they have minima at the zone boundary (the point (1,0,0)). The significance in terms of interatomic forces will now be discussed.

We now discuss a very simplified version of the Born-von Kármán theory of lattice dynamics. Consider a symmetry direction in a crystal as shown in Figure 12. For each atom on one side of the vertical, a corresponding atom is found on the other. Then by symmetry, a lattice wave propagating in the vertical direction must be either longitudinal (as shown) or transverse. Consider small displacement U_ℓ of some particular atom (ℓ) and of its neighbors (ℓ'). Then the equation of motion of the ℓ-th atom is as shown: the force on the ℓ-th atom is the sum of forces caused by the displacements U_ℓ' of its neighbors (and of itself, the sum includes the term $\ell = \ell'$). The force constant $\Phi_{\ell\ell}$ gives the force on atom ℓ in the direction considered when atom ℓ' is moved a unit distance in the same direction. It is these force constants in which we are interested.

If we substitute in the equation of motion the expression for the displacement caused by a simple traveling plane wave, we obtain an expression for the angular frequency ω in terms of the

$$M\ddot{u}_{\ell} = -\sum_{\ell'} \Phi_{\ell\ell'} u_{\ell'}$$

$$u_{\ell'} \propto \exp.\left[i\left(\vec{q}\cdot\vec{R}_{\ell} + \vec{q}\cdot\vec{R}_{\ell\ell'} - \omega t\right)\right]$$

$$M\omega^2 = \sum_{\ell'} \Phi_{\ell\ell'} \exp.\left(i\,\vec{q}\cdot\vec{R}_{\ell\ell'}\right)$$

$$= \sum_{n=1}^{N} \Phi_n \left[1 - \cos\left(\pi n q/q_M\right)\right]$$

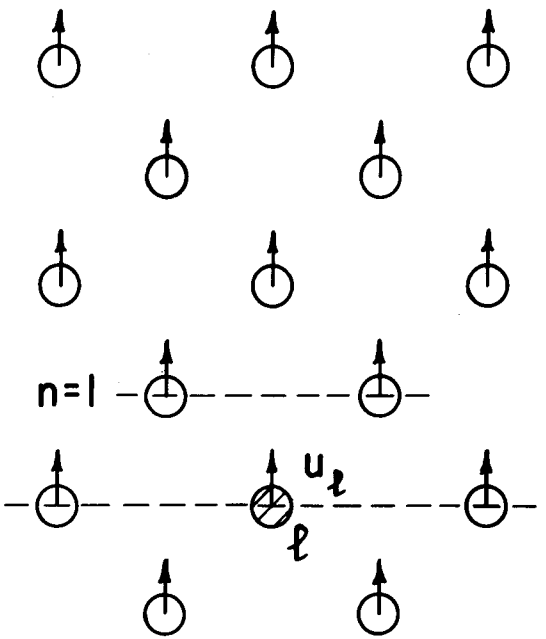

Figure 12

force constants. The phase of the wave ($\underset{\sim}{q}.\underset{\sim}{R}_{\ell\ell'}$) is constant over planes of atoms normal to $\underset{\sim}{q}$. We can, therefore, sum over the atoms in a given plane and arrive at the expression shown which indicates that the quantity mass x (angular frequency)^2 can be Fourier analyzed, the Fourier coefficients (Φ_N) being <u>linear combinations</u> of the <u>interatomic</u> force constant $\Phi_{\ell\ell'}$ and effectively force constants between <u>planes</u> of atoms. The sum over planes must be taken to a value N such that the force constant $\Phi_n = 0$ for planes n>N.

Thus, if we Fourier analyze the dispersion curves (in the form $M\omega^2$) we obtain interplanar force constants and, thus, the <u>range</u> of the interatomic forces. This was first pointed out by Foreman and Lomer[21] in 1957.

In Figure 13, we show the Fourier composition of the longitudinal waves propagating along the cube edge. The experimental values of $M\omega^2$ are shown together with least square fits involving five planes and twelve planes. With twelve planes, a good fit is, of course, obtained; with five planes, the fit is not quite so good and is probably outside the errors. The Fourier components from other planes are also shown. Clearly the forces are very complex.

Figure 14 shows the interplanar force constants plotted against the plane number and the distance between planes. It is clear that planes of atoms six planes away have an appreciable influence. The nearest atom in a plane six planes away is the

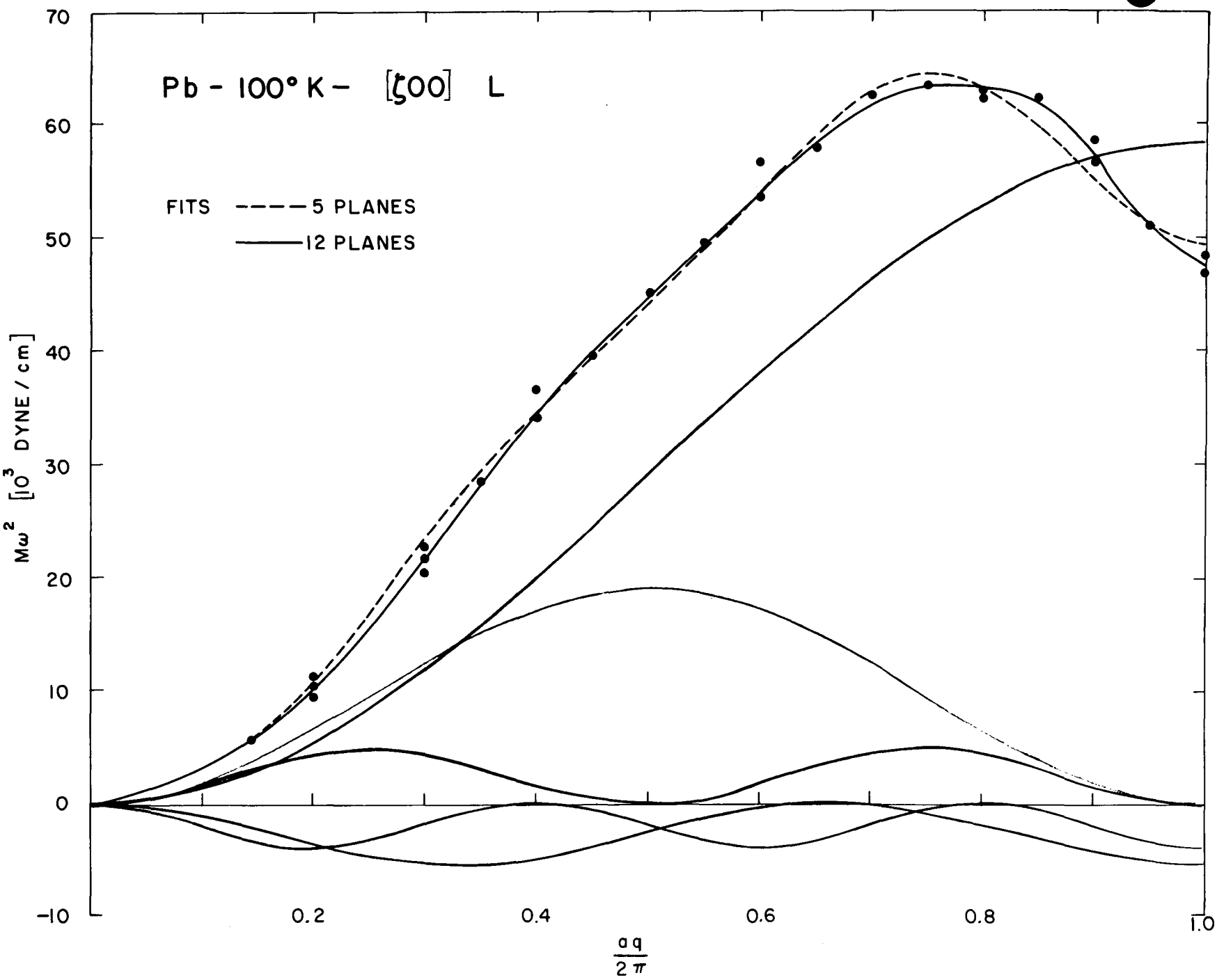
Pb - 100° K - [ζ00] L
FITS
5 PLANES
12 PLANES
70
60
50
40
30
20
10
0
-10
0.2
0.4
0.6
0.8
1.0
Mω² [10³ DYNE / cm]
aq / 2π

Figure 13

Figure 14

A.E.C.L. Ref. # A- 2751-A

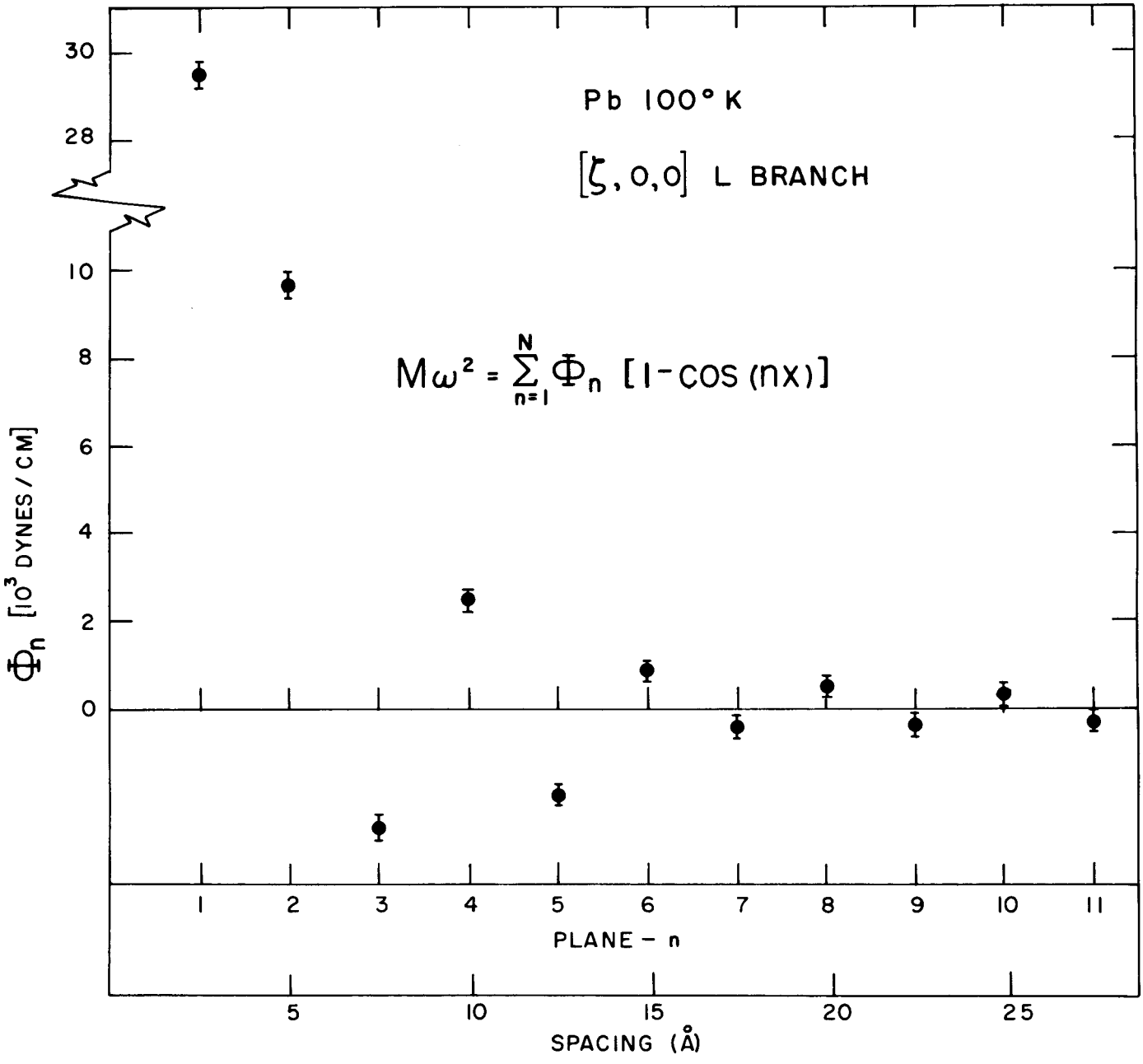

seventeenth neighbor atom. Thus, the range of forces in lead is very great indeed.

We now return to the dispersion curves of Figure 11. If we look closely at the curves, we see several small anomalies. On the theory just discussed, these would give rise to very high Fourier components and, thus, would correspond to forces between even more distant atoms.

In 1959, Kohn[22] proposed that there should exist in the dispersion curves of metals small anomalies at which the dispersion curve had a logarithmically infinite slope. The position of the anomaly was related to the position in reciprocal space of the Fermi surface of the metal.

We believe that the anomalies we observe are real, and that they are essentially the anomalies of Kohn.

Let us now consider in detail the longitudinal branch in the (111) direction of the reduced zone.

Using the constant $\underset{\sim}{Q}$ method, we march successively through points along the (111) direction of reciprocal space, which is also the (111) direction of the reduced zone, taking energy distributions at each point as shown in Figure 10. The centers of the groups give frequencies which, when plotted, show an anomaly near the zone boundary. The series was continued across the zone boundary, and the anomaly was found at the corresponding

position in the next zone.

Although the anomaly is small, we do not believe that it could arise from fluctuations in peak position due to counting statistics. However, there could conceivably be some unknown contaminant effect which shifts the position of the peaks. To check this, we repeated the experiments using other neutron energies. The results for the region of the anomaly, plotted on a large scale in the reduced zone, are shown in Figure 15.

The different runs at different energies are shown by different symbols. A and B refer to the two zones in reciprocal space shown in Figure 10. Every run showed the anomaly at roughly the same position.

In Figure 16, we show the Fermi surface of lead, in the extended zone scheme based primarily on de Haas-van Alphen measurements by A. V. Gold[23] but slightly modified to fit our results[18]. According to Kohn, anomalies occur when the phonon wave vector plus any reciprocal lattice vector just equals a diameter of the Fermi surface. The phonon can then cause large numbers of almost elastic virtual electron scatterings with a consequent modification of the frequency of the phonon.

The Fermi surface is based on the free electron surface containing four electrons, shown as the circle in Figure 16. The anomaly shown in Figure 15 can be identified with the Kohn anomaly produced by scattering electrons with wave vector

Figure 15

A.E.C.L. Ref. # A-2733-K

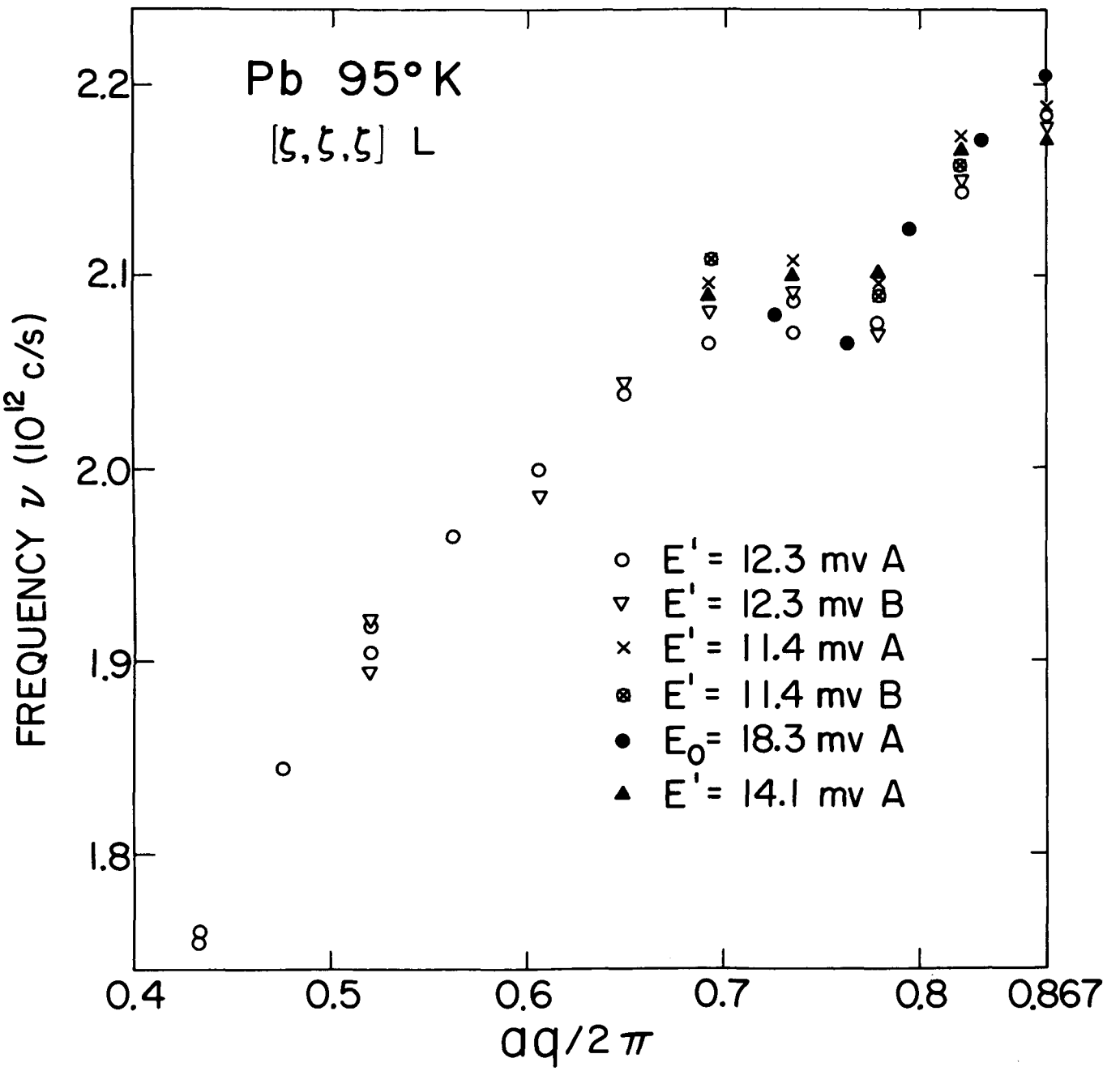

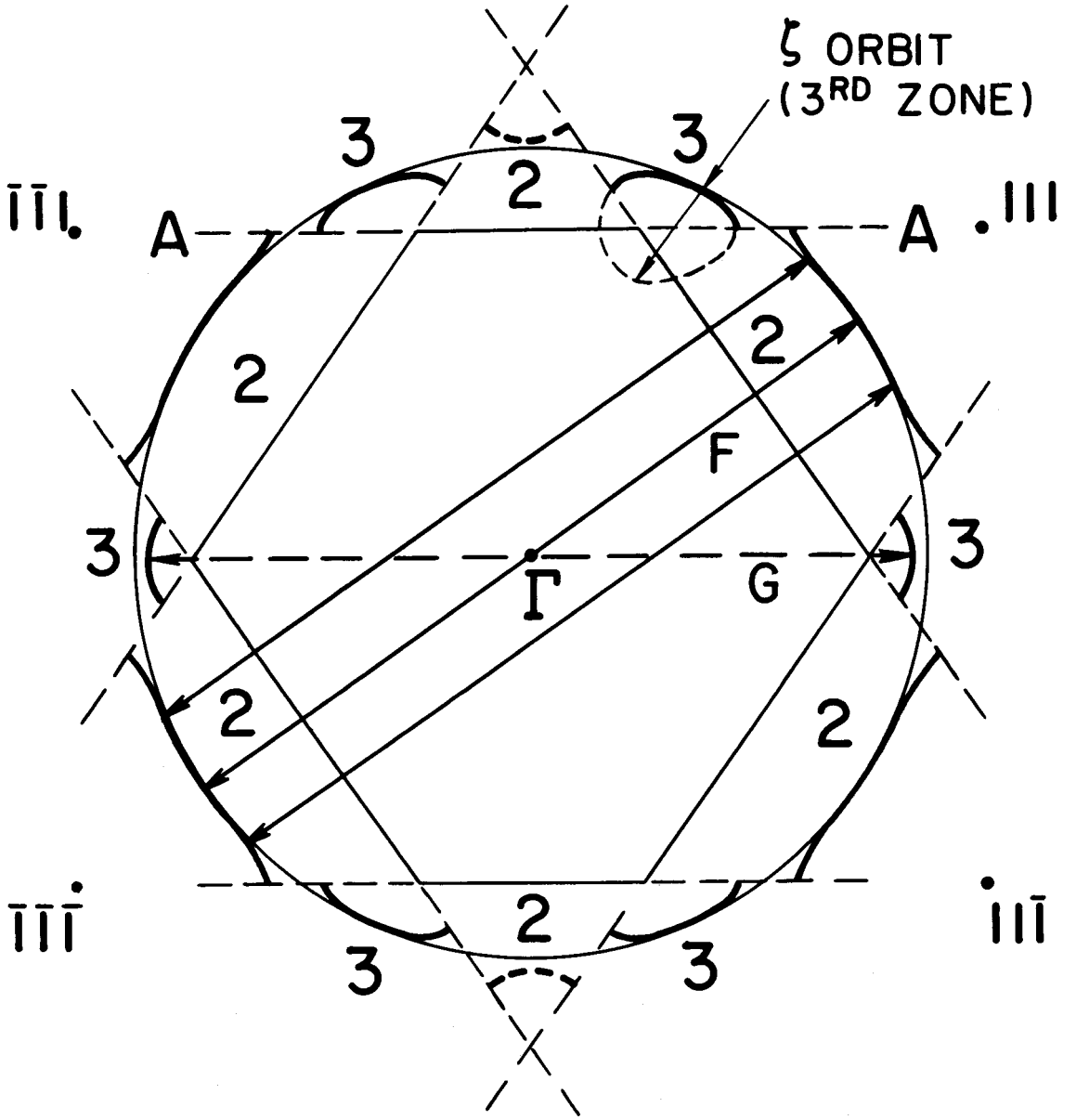

Figure 16

transfers marked F. If this identification is made, the diameter of the real Fermi surface is found to be no more than 1% greater than the diameter of the free electron surface (in the (111) direction in the extended zone scheme).

In the (110) direction, we also see an anomaly which can be identified with the Kohn anomaly marked G. For this case, the anomaly indicates that the diameter is about 4% smaller than the free electron diameter. This is in excellent agreement with the de Haas-van Alphen effect measurements of Gold, who found that the closely related orbits in the third zone have the area shown, about 1/3 smaller than for free electrons.

The anomaly we identify with the Kohn anomaly G of Figure 16 is indicated by the arrow in Figure 17. For free electrons, its position would have been as given by the dotted arrow. Again, the anomaly was checked by studying it along several different lines through reciprocal space, and again it appeared in each experiment.

To sum up: In lead, we have forces extending to very great distances; these forces seem to arise from details of the electronic structure and show evidence of the influence of the Fermi surface.

Lead is a substance in which there is a strong electron-phonon interaction. This is jargon which expresses the fact that the wave functions of the electrons in lead are strongly affected by the positions of the ions. Correspondingly, the detailed behavior of

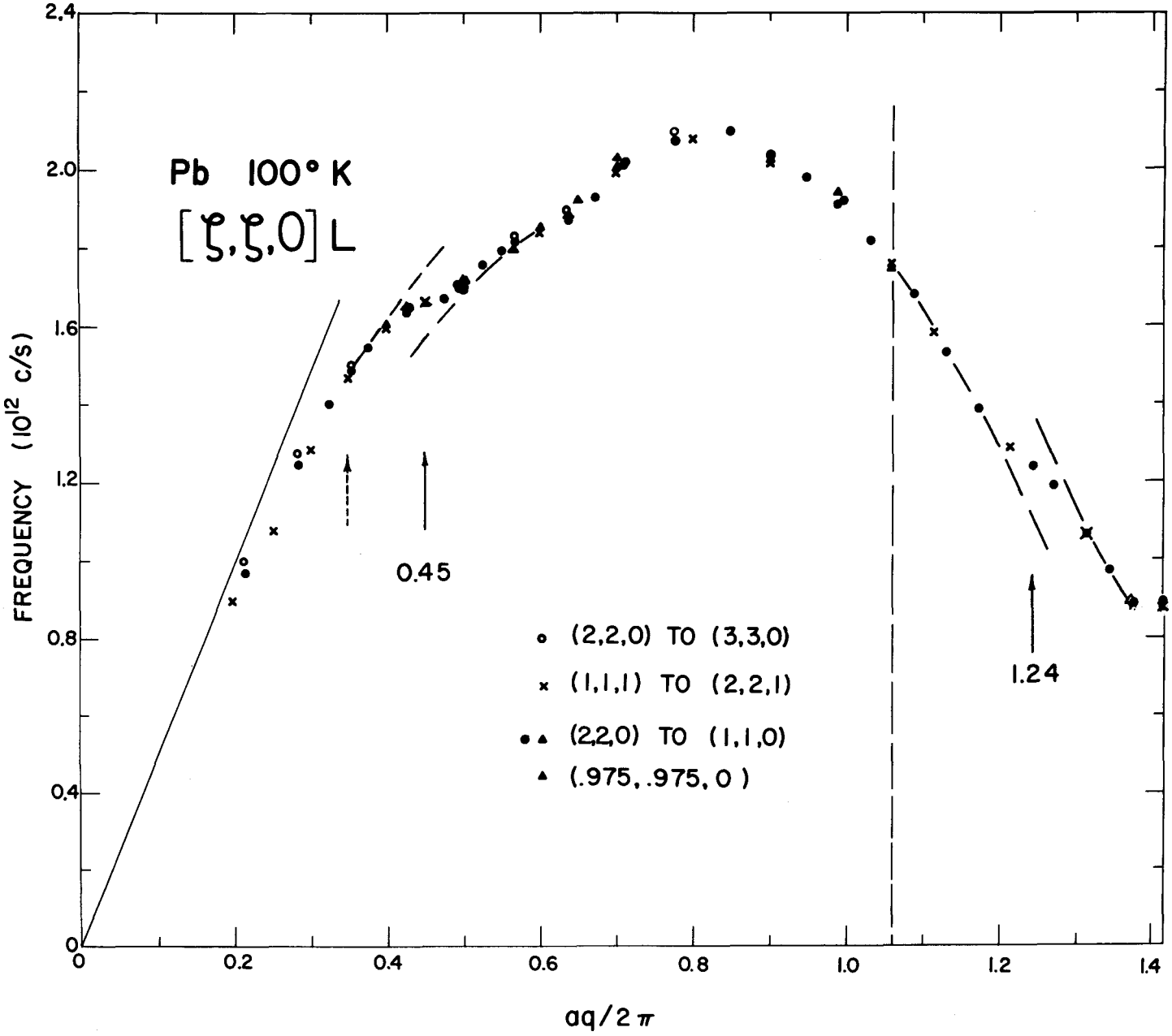
Pb 100° K
[ζ,ζ,0] L
FREQUENCY (10^{12} c/s)
aq/2π
0.45
1.24
(2,2,0) TO (3,3,0)
(1,1,1) TO (2,2,1)
(2,2,0) TO (1,1,0)
(.975, .975, 0)
0
0.2
0.4
0.6
0.8
1.0
1.2
1.4
1.6
1.8
2.0
2.4

Figure 17

the conduction electrons has an important influence on the lattice vibrations.

We have also studied[19,20] another metal---sodium---in which the electron-phonon interaction is small. In sodium, the conduction electrons are spread out almost uniformly through the crystal, and are comparatively little affected by the positions of the ions. Correspondingly, the influence of the details of the electronic structure on the lattice vibrations is smaller than in lead.

These remarks can be made more quantitatively[18] in terms of the electron-phonon matrix element of Bardeen and calculations of Toya[24].

Measurements were carried out[19,20] on a sodium crystal at liquid nitrogen temperature with Dr. Woods, Dr. A. T. Stewart and Mr. R. H. March, in collaboration with Dr. Raymond Bowers of Cornell University who grew the very large crystals used. The results for three symmetric directions are shown in Figure 18. Many other measurements were also made.

The solid curves are theoretical calculations of Toya[24], published in 1958 in a Japanese journal---The Journal of the Institute of Catalysis of Hokkaido University. Toya solved the Hartree-Fock equations of the metal in the presence of lattice vibrations. His equations exhibit <u>explicitly</u> the Kohn effect, although he did not comment on this, and indeed the anomalies are very small in sodium. (We searched for the anomalies at a number of places at which they

Figure 18

A.E.C.L. Ref. # A-2721-F

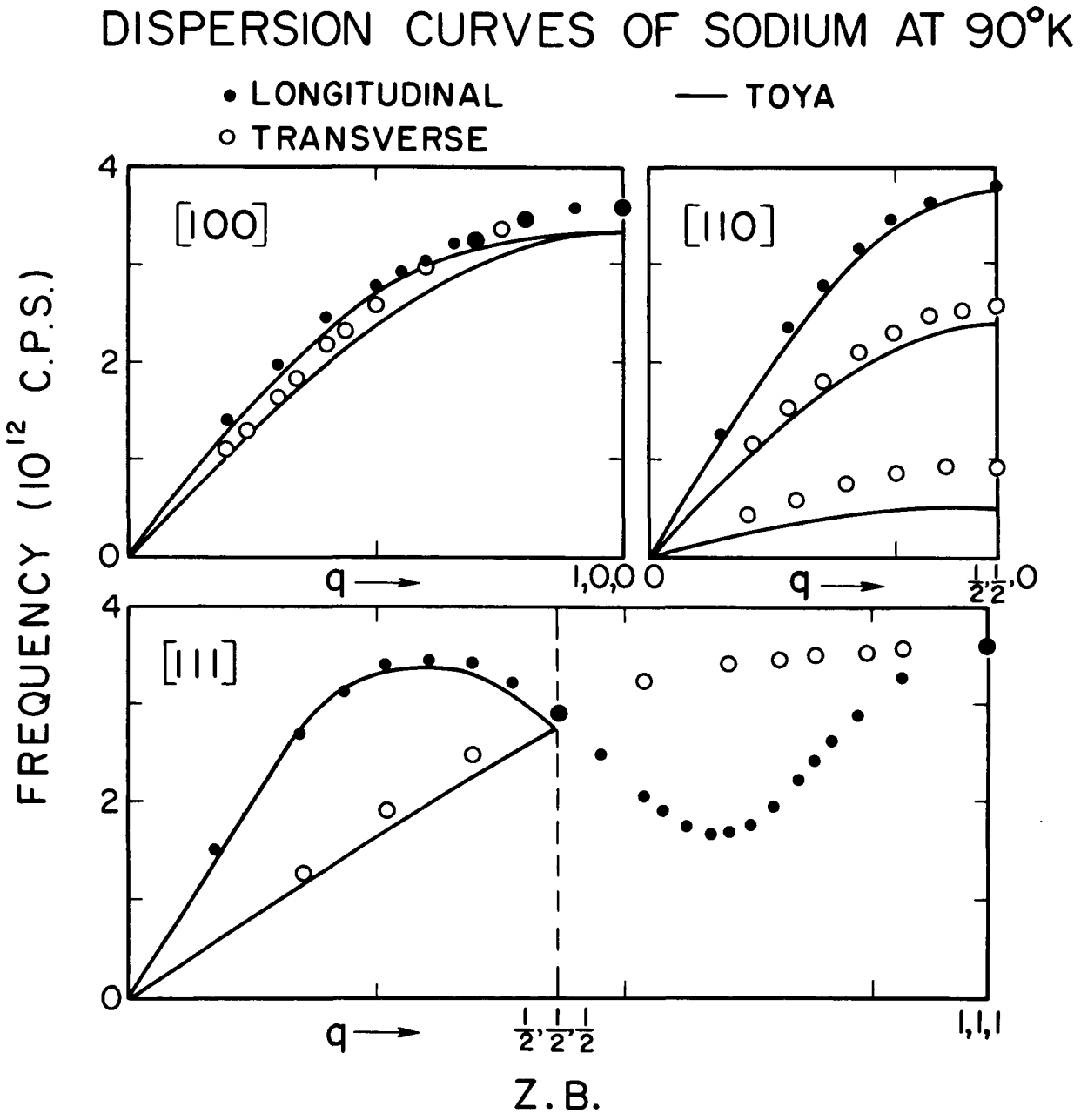

would occur for free electrons without result; they are, in fact, small).

The agreement of Toya's calculations with experiment is quite good, considering that no fitting whatever was involved. We have analyzed the experiments in terms of the Born-von Kármán theory and have determined the interatomic force constants in the metal. In contrast to lead, the forces are of comparatively short range: they extend to fifth neighbors only (or perhaps a trifle farther), and a qualitative fit can be obtained using first and second neighbors only. The forces have been found to be substantially central, and can probably be derived from a potential with fair accuracy.

Up to this point, we have been considering ideal harmonic non-interacting normal modes. But, as evidenced by such effects as thermal expansion, the normal modes do interact, causing the phonons to have a finite lifetime. The phonon lifetime is reflected through the uncertainty principle in an energy broadening of the neutron groups.

In Figure 19, we see an example of a neutron group[25]; at low temperatures, it has probably just the resolution width; at room temperature, the group has broadened and shifted in frequency. At the right, we see the energy broadening, plotted against the reduced wave vector, for the (110) transverse branch. This broadening is quite large: at the zone boundary, the corresponding lifetime

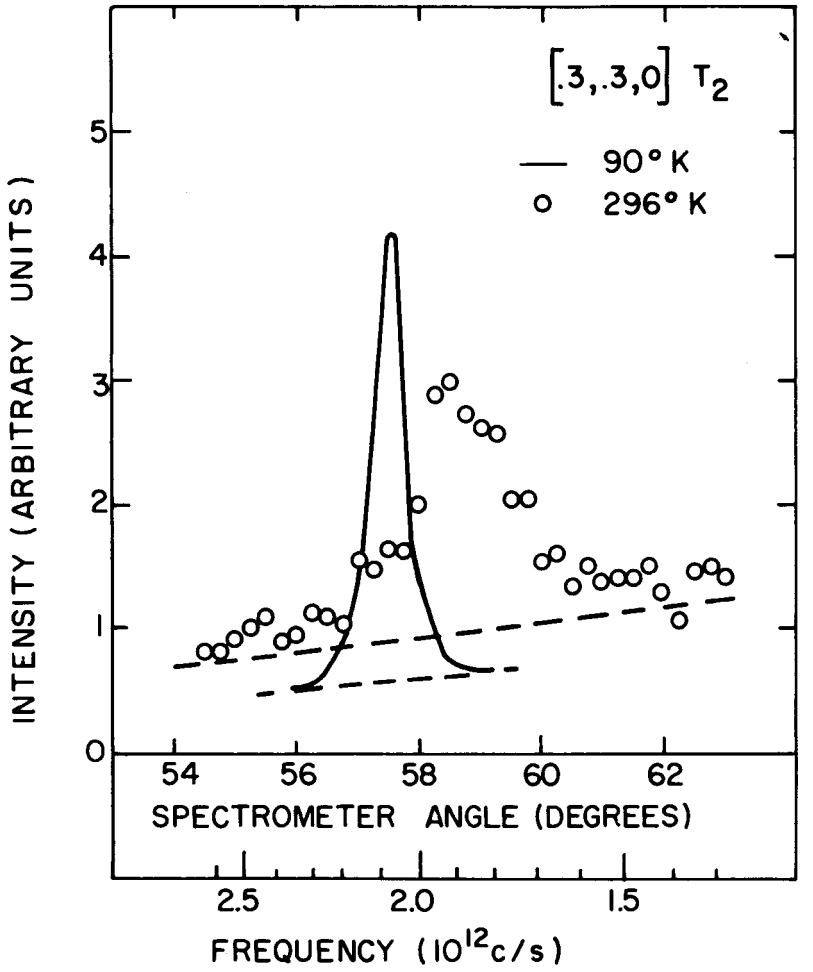
[.3,.3,0] T2
90° K
296° K
INTENSITY (ARBITRARY UNITS)
0
1
2
3
4
5
54
56
58
60
62
SPECTROMETER ANGLE (DEGREES)
2.5
2.0
1.5
FREQUENCY (10^12 c/s)

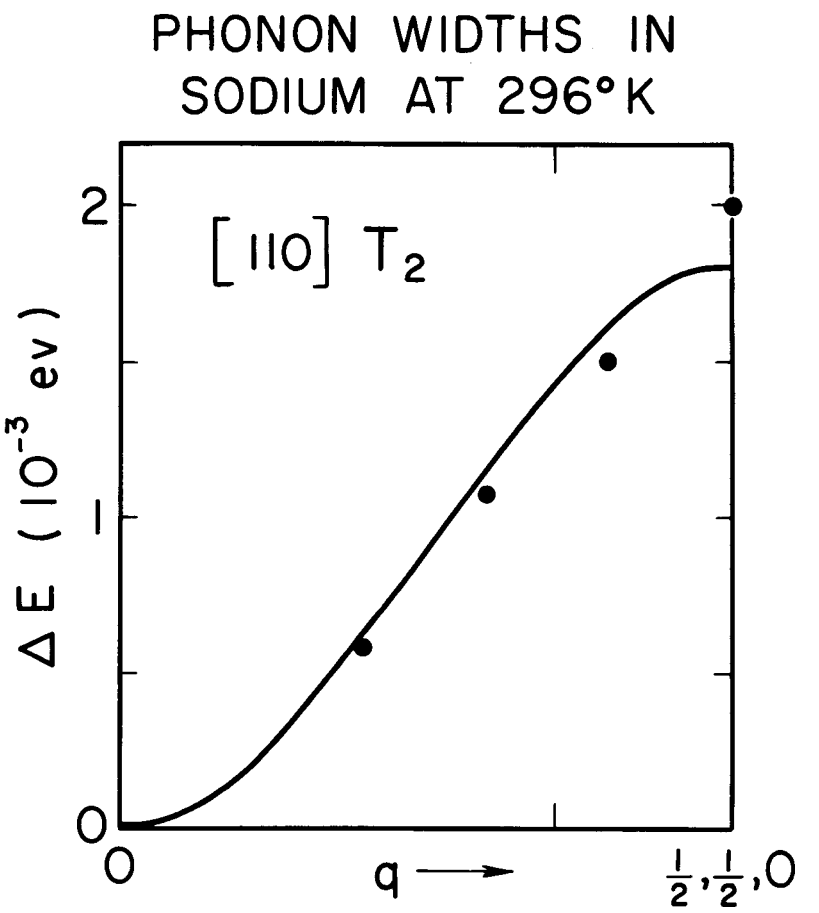
PHONON WIDTHS IN
SODIUM AT 296° K
[110] T2
ΔE (10^-3 ev)
0
1
2
0
q
1/2, 1/2, 0

Figure 19

is only slightly longer than the period of the vibration. Such extra-ordinarily short phonon lifetimes were previously found by our group[16] in lead and, independently, by Larson, Dahlborg and Holmryd[11] at Stockholm, in aluminum.

In the last few pages, I would like to discuss the dispersion relation of the spin waves in crystals. In neutron diffraction, the time-independent aspects of the magnetic structure of materials is studied. Neutron inelastic scattering gives access to the magnetic dynamics of the material, the behavior of the magnetic structure in time.

An aligned magnetic system has a set of normal modes---the spin waves---which behave in scattering neutrons much like the lattice vibrations. In particular, one-quantum scattering occurs in an exactly analogous way to one-phonon scattering and results in neutron groups which can be used to determine the dispersion relation for the spin waves.

The neutron groups produced by spin waves can be distinguished from those produced by phonons by the behavior of the intensities when the spin system is reoriented by application of a magnetic field, that is, the magnon neutron groups have a characteristic magnetic signature.

Experiments on magnetic inelastic spin wave scattering were first done by R. D. Lowde[26] (at Harwell about 1955), who studied the diffusely scattered intensity without performing energy analysis.

Experiments on magnetite[27] carried out at Chalk River in 1956 demonstrated the applicability of the conservation laws to spin wave scattering, and thus, the reality of the spin wave quantum---the magnon---and gave a crude partial dispersion curve for the acoustic magnons (Figure 20).

In 1960, the dispersion curve of the spin waves in a metal---a face central cubic alloy of cobalt with 8% iron---was determined[28] by R. N. Sinclair and myself as shown in Figure 21. The quadratic relation between the quantum energy and the wave vector, which is characteristic of ferromagnetic spin waves, was obtained. The dispersion curve could not be followed to higher energies because of the limited range of neutron energies available in the Maxwellian spectrum from the reactor. This curve is certainly among the most cogent evidence for the existence of spin waves in metals.

Very recently, the study of the spin wave in magnetite has been taken up again, in collaboration with Dr. Hiroshi Watanabe from Tohoku University. In this work so far, the complete acoustic dispersion curve and a part of one optical spin wave branch has been measured[29] as shown in Figure 22. Although a complete analysis has not been carried out, the results so far are substantially in agreement with the Néel theory of ferrites and with current ideas on the spin wave spectrum due to Kouvel[30], Kaplan[31] and others. The results indicate a large J_{AB} interaction ($\sim 2.3 \times 10^{-3}$ ev) and probably much smaller values for J_{AA} and J_{BB}. A complete analysis of these and other results would probably enable

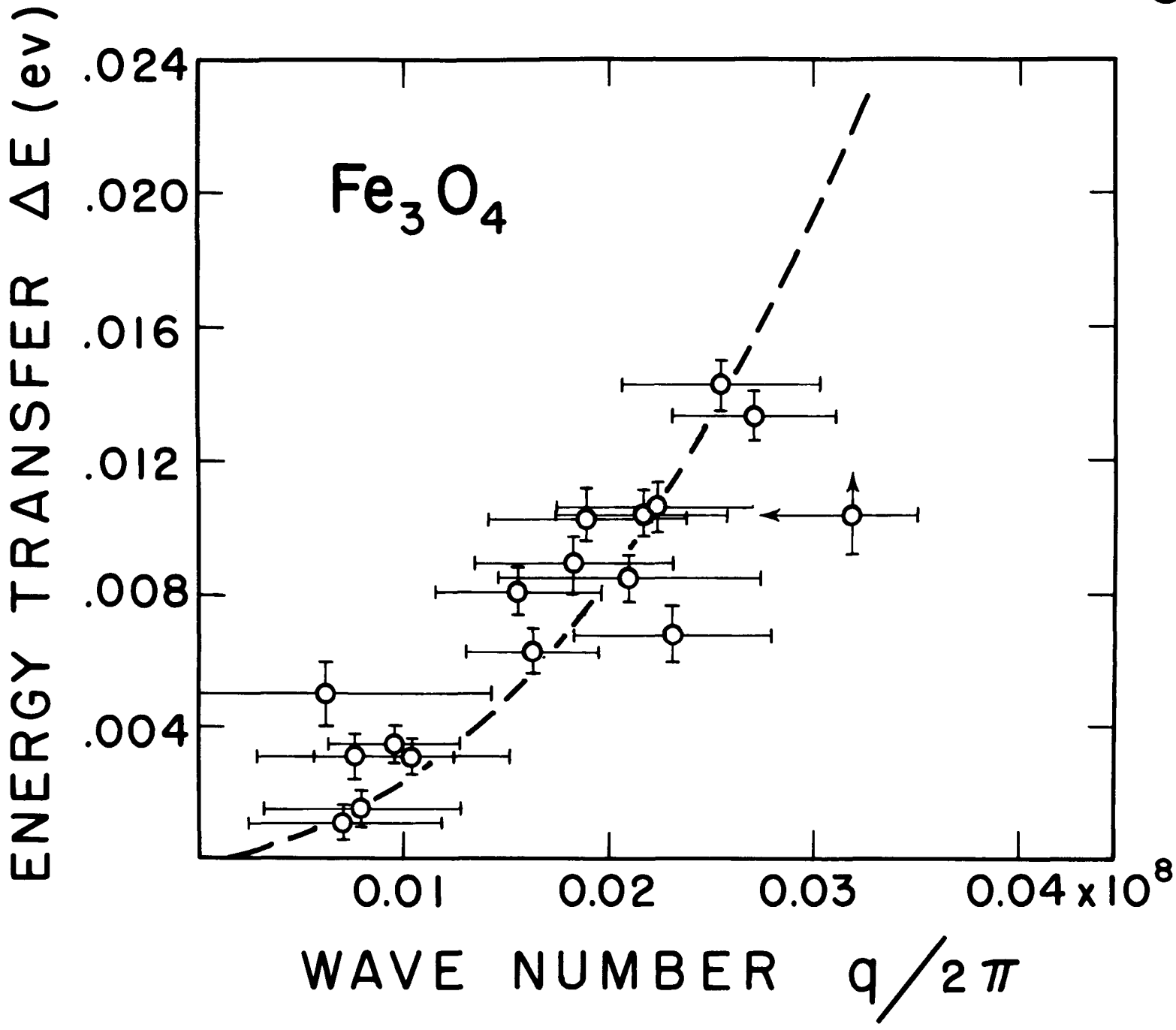
ENERGY TRANSFER ΔE (ev)
.024
.020
.016
.012
.008
.004
Fe_3O_4
0.01
0.02
0.03
0.04 x 10^8
WAVE NUMBER q/2π

Figure 20

Figure 21

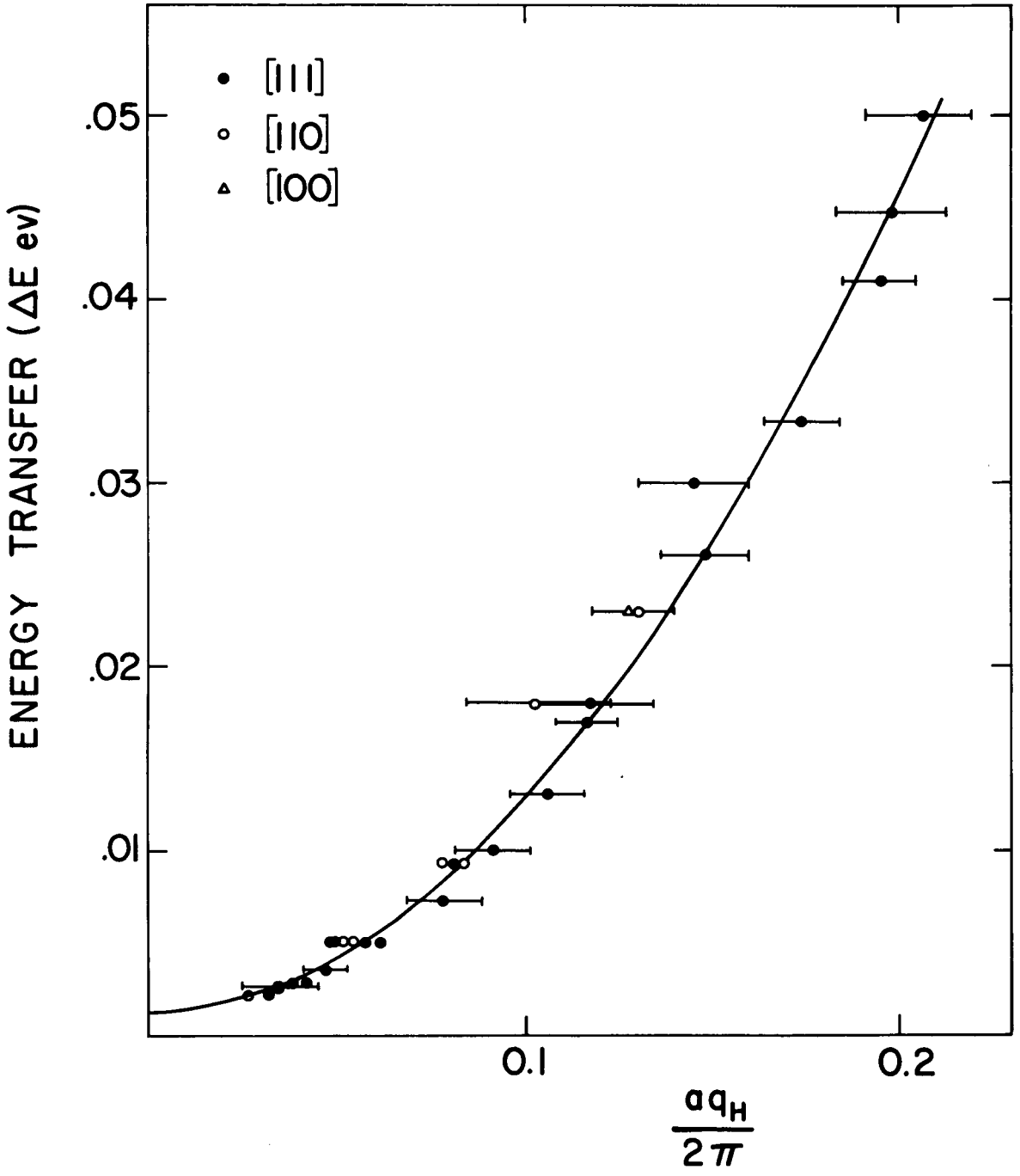
[111]
[110]
[100]
.05
.04
.03
.02
.01
ENERGY TRANSFER (ΔE ev)
0.1
0.2
$\frac{aq_H}{2\pi}$

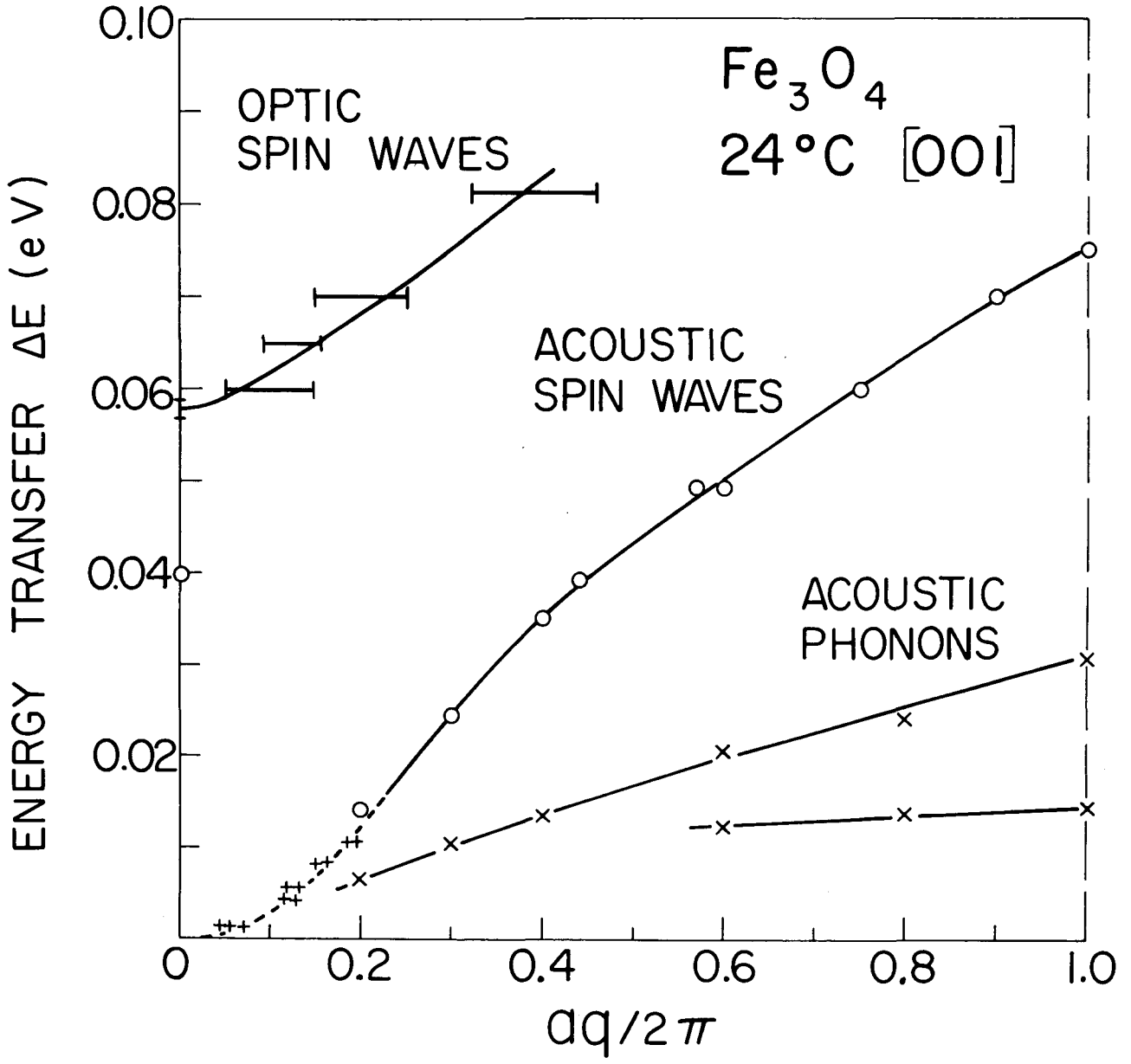
Fe_3O_4
24°C [001]
OPTIC
SPIN WAVES
ACOUSTIC
SPIN WAVES
ACOUSTIC
PHONONS
ENERGY TRANSFER ΔE (eV)
0.10
0.08
0.06
0.04
0.02
0
0.2
0.4
0.6
0.8
1.0
aq/2π

Figure 22

good values for these interaction constants to be obtained and would also provide a rigorous check on the validity of the general picture.

This concludes the paper. The experiments take a considerable length of time, but we can look forward, over the next few years, to rather accurate measurements on the dispersion curves for both the lattice vibrations and the spin waves in most simple materials. This should lead to greatly improved understanding of the interactions between the atoms in crystals.

References

1. J. M. Cassels and R. Latham, Phys. Rev., 74, 103 (1948).

2. P. A. Egelstaff, Nature, 168, 290 (1951).

3. B. N. Brockhouse and D. G. Hurst, Phys. Rev., 88, 542 (1952).

4. B. N. Brockhouse, Phys. Rev., 98, 1171A (1955).

5. R. Weinstock, Phys. Rev., 65, 1 (1944).

6. G. H. Begbie and M. Born, Proc. Roy. Soc. (London), A188, 179 (1946). M. Born and K. Huang, Dynamical Theory of Crystal Lattices, Oxford University Press, New York (1954).

7. B. N. Brockhouse and P. K. Iyengar, Phys. Rev., 111, 747 (1958).

8. Reported at the Royal Society of Canada in June 1955; issued as Unpublished Report AECL 221.

9. B. N. Brockhouse and A. T. Stewart, Phys. Rev., 100, 756 (1955); Revs. Modern Phys., 30, 236 (1958).

10. R. S. Carter, D. J. Hughes and H. Palevsky, Phys. Rev., 106, 1168 (1957).

11. K. E. Larsson, U. Dahlborg and S. Holmryd, Ark. Fys., 17, 369 (1960).

12. C. B. Walker, Phys. Rev., 103, 547 (1956).

13. W. Cochran, Proc. Roy. Soc., A253, 260 (1959).

14. R. J. Collins and H. Y. Fan, Phys. Rev., 93, 674 (1954); W. G. Simeral, thesis, University of Michigan, unpublished.

15. B. N. Brockhouse in Inelastic Scattering of Neutrons in Solids and Liquids, I.A.E.A., Vienna, 113 (1961).

16. B. N. Brockhouse, T. Arase, G. Caglioti, M. Sakamots, R. N. Sinclair and A. D. B. Woods, p. 531, ref. 15.

17. B. N. Brockhouse, K. R. Rao and A. D. B. Woods, Phys. Rev. Letters, 7, 93 (1961).

18. B. N. Brockhouse, T. Arase, G. Caglioti, K. R. Rao and A. D. B. Woods, Phys. Rev.

19. A. D. B. Woods, B. N. Brockhouse, R. H. March and R. Bowers, Proc. Phys. Soc. (London), 79, 440 (1962).

20. A. D. B. Woods, B. N. Brockhouse, R. H. March A. T. Stewart and R. Bowers, Phys. Rev.

21. A. J. E. Foreman and W. M. Lomer, Proc. Phys. Soc. (London), B70, 1143 (1957).

22. W. Kohn, Phys. Rev. Letters, 2, 393 (1959).

23. A. V. Gold, Trans. Roy. Soc. (London), A251, 85 (1958).

24. T. Toya, J. Res. Inst. for Catalys. Sapporo, 6, 183 (1958).

25. A. D. B. Woods and B. N. Brockhouse, unpublished.

26. R. D. Lowde, Proc. Roy. Soc., A235, 305 (1956).

27. B. N. Brockhouse, Phys. Rev., 106, 859 (1957); Phys. Rev., 111, 1273 (1958).

28. R. N. Sinclair and B. N. Brockhouse, Phys. Rev., 120, 1638 (1960).

29. H. Watanabe and B. N. Brockhouse, Physics Letters, 1, 189 (1962).

30. J. S. Kouvel, Tech. Rept. No. 210, Cruft Laboratory, Harvard University (1955).

31. T. A. Kaplan, Phys. Rev., 109, 782 (1958).